Neuron, Vol. 34, 945–960, June 13, 2002, Copyright ©2002 by Cell Press

Coordinated Interaction of Neurogenesis and Angiogenesis in the Adult Songbird Brain

Abner Louissaint, Jr., Sudha Rao, Caroline Leventhal, and Steven A. Goldman[1]
Department of Neurology and Neuroscience
Cornell University Medical Center
1300 York Avenue
New York, New York 10021

Summary

Neurogenesis proceeds throughout life in the higher vocal center (HVC) of the adult songbird neostriatum. Testosterone induces neuronal addition and endothelial division in HVC. We asked if testosterone-induced angiogenesis might contribute importantly to HVC neuronal recruitment. Testosterone upregulated both VEGF and its endothelial receptor, VEGF-R2/Quek1/KDR, in HVC. This yielded a burst in local HVC angiogenesis. FACS-isolated HVC endothelial cells produced BDNF in a testosterone-dependent manner. In vivo, HVC BDNF rose by the third week after testosterone, lagging by over a week the rise in VEGF and VEGF-R2. In situ hybridization revealed that much of this induced BDNF mRNA was endothelial. In vivo, both angiogenesis and neuronal addition to HVC were substantially diminished by inhibition of VEGF-R2 tyrosine kinase. These findings suggest a causal interaction between testosterone-induced angiogenesis and neurogenesis in the adult forebrain.

Introduction

The vocal control nucleus HVC of adult songbirds generates and recruits new neurons throughout life (Goldman and Nottebohm, 1983; Nottebohm, 1985). The integration and survival of these neurons is modulated by the gonadal steroids testosterone and estradiol (Hidalgo et al., 1995; Johnson and Bottjer, 1995; Nordeen and Nordeen, 1989; Rasika et al., 1994), whose actions mediate the seasonal hypertrophy of HVC in adult canaries (Nottebohm, 1981). Notably, estrogen and testosterone are also associated with accentuated angiogenesis in the adult female canary HVC (Goldman and Nottebohm, 1983; Hidalgo et al., 1995). Testosterone treatment in particular yielded a >25-fold increase in the [^{3}H]thymidine-determined mitotic index of HVC endothelial cells. This burst of endothelial cell division was transient and self-limited; endothelial mitotic indices fell to baseline within 2 weeks after testosterone implantation, despite persistently elevated androgen levels during that period (Goldman and Nottebohm, 1983).

We became intrigued about the concurrence of gonadal steroid treatment with both neuronal recruitment and angiogenesis in the adult HVC and sought to establish the nature of their coassociation. Specifically, we asked whether androgen-associated endothelial proliferation might contribute to the acceptance of newly generated neurons by adult brain parenchyma. Certainly, brain endothelial cells may be targets of systemic gonadal steroids (Goldman and Nottebohm, 1983; Hidalgo et al., 1995), and testosterone in particular appears to induce endothelial cell division in precisely those regions of the neostriatum into which new neurons are recruited (Goldman and Nottebohm, 1983). This seemed unlikely to be coincidental; endothelial cells (ECs) can serve as potent sources of secreted chemokines and trophic agents. These include FGF2 and IGF1 (Biro et al., 1994), which are potent mitogens for neural progenitor cells (Drago et al., 1991; Gensburger et al., 1987), and PDGF and IL-8, which may act as differentiation and survival factors, respectively, for newly generated neurons (Araujo and Cotman, 1993; Johe et al., 1996). Of particular interest, human brain endothelial cells can secrete brain-derived neurotrophic factor (BDNF) (Leventhal et al., 1999) in quantities sufficient to support neuronal differentiation from the adult rat forebrain ventricular zone (Kirschenbaum and Goldman, 1995; Leventhal et al., 1999). This observation is particularly germane in the adult HVC, in which testosterone's neurotrophic effects may be mediated through a regional induction of BDNF, perhaps acting as a downstream effector (Rasika et al., 1994, 1999).

On the basis of these observations, we asked whether the trophic effects of gonadal steroids in the adult HVC might be mediated through the endothelial release of neurotrophic cytokines, and if so, whether neuronal addition to the adult HVC might depend upon antecedent endothelial cell activation and division. We report that testosterone treatment of the adult female canary, which can trigger primitive song in these otherwise nonsinging birds, induces the rapid production of both vascular endothelial growth factor (VEGF) and its receptor, VEGFR2/KDR/Quek1 in nucleus HVC. This leads to rapid endothelial cell division, which in turn predicts the regionally restricted expansion of the HVC capillary vasculature. The newly activated and expanded vasculature substantially increases its production and release of BDNF, whose induction is both spatially and temporally associated with the recruitment of new neurons to HVC. By this means, gonadal steroids may act upon the local microvascular bed to provide a permissive environment for neuronal recruitment into the adult songbird brain.

Results

Testosterone Induces Mitotic Angiogenesis in the Adult Canary HVC

Testosterone treatment substantially increases the proliferation rate of HVC endothelial cells (Goldman and Nottebohm, 1983). This finding suggested that testosterone might directly induce mitotic angiogenesis in the adult HVC. To test this possibility, we first set about to confirm that testosterone could indeed induce endothelial cell division in the adult HVC (Figures 1A and 1B). A cohort of six 1-year-old female canaries was implanted with either testosterone or cholesterol-containing silas-

[1]Correspondence: sgoldm@mail.med.cornell.edu

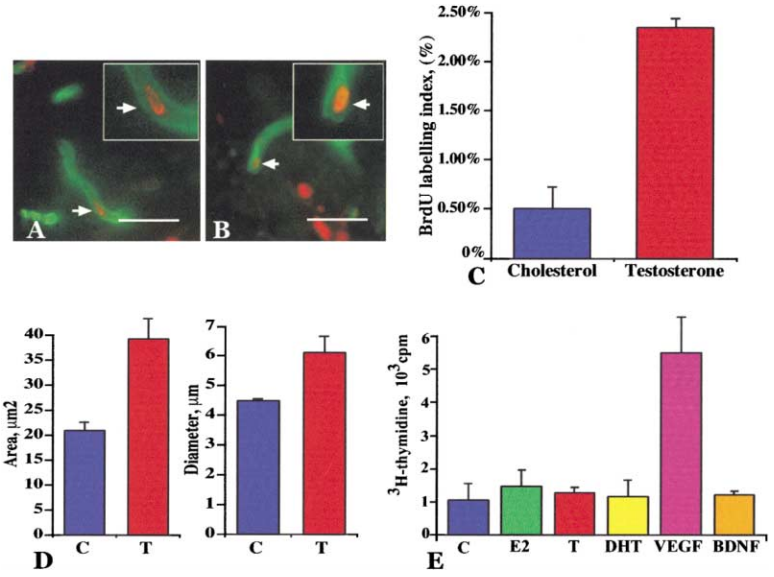

Figure 1. Testosterone Increases Mitotic Angiogenesis and Capillarization in the Adult HVC

(A and B) Representative high-power images of BrdU$^+$ (red)/laminin$^+$ endothelial cells (green) in a testosterone-treated adult female canary HVC. This bird was killed 7 days after hormone-silastic implant and immediately after 2 days of bidaily injections of BrdU. Double-labeled cells in the testosterone-treated HVC are indicated with arrows.

(C) This plot compares the difference in the HVC endothelial labeling index, defined as the fraction of BrdU$^+$/laminin$^+$ cells among all laminin$^+$ HVC endothelial cells, between testosterone-treated birds and their cholesterol-treated controls.

(D) These plots compare the average area and diameter of laminin$^+$ vessels in the HVCs of testosterone- and cholesterol-treated female canaries. Each parameter was significantly greater in the testosterone-treated birds than in their controls.

(E) This graph plots the effect of cholesterol (C), estradiol (E2), testosterone (T), and dihydrotestosterone (DHT), as well as that of VEGF and BDNF, on [^{3}H]thymidine incorporation by HVC/MCN endothelial cells in vitro. Neither androgens nor estrogen elicited any significant increase in [^{3}H]thymidine incorporation by these cells. In contrast, VEGF addition was associated with a statistically significant ($p < 0.001$), >5-fold increase in net [^{3}H]thymidine incorporation over the 48 hr test period. Thus, VEGF can act directly on HVC endothelial cells to elicit their division, whereas the gonadal steroids are not directly mitogenic for these cells. Scale = 50 μm.

tic implants (n = 3 each). This treatment has been shown to yield supraphysiological steroid levels within 24 hr of implantation (Legan et al., 1975). Beginning on the second day thereafter, the birds were injected daily for 7 days with bromodeoxyuridine (BrdU; 100 mg/kg intrapectoral) and sacrificed on day 10, a day after the last BrdU injection. Their brains were cryosectioned at 14 μm and double-immunostained for BrdU and laminin, which is selectively expressed by endothelial cells (ECs) of the HVC capillary vasculature (Alitalo et al., 1982). In each HVC, the incidence of laminin$^+$/BrdU$^+$ cells and the ratio of laminin$^+$/BrdU$^+$ cells to total HVC laminin$^+$ ECs were determined bilaterally in each of six sections spaced 200 μm apart. For total endothelial counts, individual ECs were defined by double-labeling with the nuclear dye Hoechst 33258 and laminin.

Using this protocol, we found that testosterone-treated birds had an HVC endothelial cell labeling index of 2.34% ± 0.09% (n = 3 birds, at 12 HVC samples/bird), which reflected 68 BrdU$^+$/laminin$^+$ cells among a total of 2805 laminin$^+$/Hoechst$^+$ endothelial cells in the 36 scored sections (Figure 1C). This was substantially greater than the 0.50% ± 0.32% mitotic index of the cholesterol-treated controls, in which 11 BrdU$^+$/laminin$^+$ cells were found among a total of 2910 laminin$^+$/Hoechst$^+$ cells. The stimulatory effect of testosterone on the mitotic index of HVC endothelial cells was highly significant ($p = 0.0007$ by Student's two-tailed t test), confirming that testosterone stimulated endothelial cell division in the adult female HVC.

Testosterone Treatment Results in the Expansion of the HVC Microvasculature

We next asked whether testosterone-associated endothelial cell division was accompanied by an expansion of the HVC microvasculature. Specifically, we asked whether androgen treatment was accompanied by an increment in HVC capillary number, cross-sectional area and perimeter, or luminal diameter. Two additional groups of adult female canaries (n = 3 each) were implanted with either testosterone or cholesterol-containing silastic implants and then sacrificed 21 days later, and their HVCs were analyzed for these capillary morphometrics. From each of these brains, a set of ten coronal 12 μm cryostat sections, taken as every tenth section so as to span the HVC, were cut and stained for capillary laminin. The number of capillary profiles as well as each vessel's perimeter, cross-sectional area, and luminal diameter were then measured in each HVC.

We found that both the mean capillary area and perimeter increased significantly with testosterone. The mean area of each laminin$^+$ capillary profile rose from 20.9 ± 1.6 μm^2 (n = 2037 capillary profiles in 42 fields) to 39.2 ± 4.1 μm^2 (n = 2085) ($p = 0.007$ by Student's two-tailed t test) while the mean perimeter increased from 21.0 ± 0.5 μm to 28.4 ± 0.8 μm ($p = 0.006$). Similarly, the average diameter of each vessel was significantly larger in the testosterone-treated birds (6.1 ± 0.5 μm) than in the cholesterol controls (4.5 ± 0.08 μm) ($p = 0.02$) (Figure 1D). In contrast, the number of vessel profiles/mm^2 did not differ between the testosterone-treated and control HVCs (n = 48.4 ± 7.7 and 48.1 ± 5.1 vessels/field, respectively; $p = 0.98$; each field measured 7.3 × 10^4 μm^2, so that the respective vessel counts/area were 663 and 659 vessels/mm^2). Together, these data indicated that testosterone induced both endothelial cell division and expansion of the capillary microvasculature in the adult canary HVC. This occurred without any concomitant increase in capillary number, suggesting that testosterone induced capillary expansion without vasculogenic budding.

VEGF Is Produced by the Testosterone-Stimulated HVC

To investigate the humoral basis for testosterone-modulated angiogenesis in the adult HVC, we next probed the testosterone-stimulated female canary brain for vascular endothelial growth factor (VEGF). VEGF is an endothelial cell mitogen that can be secreted by most somatic cell types (Leung et al., 1989). Androgen-induced VEGF expression has previously been noted by prostatic fibroblasts (Levine et al., 1998) and by murine mammary carcinoma cells (Jain et al., 1998). In the CNS, VEGF is synthesized and secreted by the developing neuroectoderm, which may utilize it to attract and expand capillary ingrowth (Breier et al., 1992). In the postnatal brain, VEGF transcripts have been identified in both astrocytes and neurons (Ogunshola et al., 2000), by which means brain VEGF—despite a decline after early development—is expressed throughout life. Yet despite VEGF's persistence in the brain (Robertson et al., 1985), and notwithstanding several reports that its exogenous administration can induce CNS angiogenesis (Rosenstein et al., 1998; Yancopoulos et al., 2000), the role of endogenous VEGF in the regulation of angiogenesis in the normal adult CNS has never been studied.

To determine if testosterone induced VEGF in the adult HVC, we treated six adult female canaries with implants of either testosterone or cholesterol ($n = 3$ each) and assessed HVC VEGF mRNA levels thereafter. Whereas only trace levels of VEGF mRNA were detected in cholesterol-treated control HVCs, VEGF mRNA was readily demonstrable by both RT-PCR and in situ hybridization within 4 days of testosterone implantation (Figures 2A and 2B). At that time point, even though little or no VEGF mRNA could be detected in cholesterol-treated HVCs after 36 cycles of PCR, VEGF mRNA was readily detected in testosterone-treated HVC after 24 cycles, and was pronounced by 30. The resultant difference in VEGF mRNA levels between testosterone-stimulated and control HVC was consistent among the three pairs of treated birds and their matched controls (Figure 2B). Thus, testosterone treatment yielded the rapid induction of VEGF mRNA expression in HVC.

Testosterone-Induced VEGF Synthesis Preceded Angiogenesis

We had previously noted that endothelial cell mitotic indices rose significantly within 6 days of testosterone administration and peaked 9–10 days after the onset of treatment (Goldman and Nottebohm, 1983). In the present study, we predicted that the androgen-induced surge in VEGF would precede androgen-induced angiogenesis and hence be even more rapid in onset. To define the time course of VEGF induction by testosterone, we prepared a set of 15 birds with testosterone implants on day 0, and we sacrificed 3 birds each on days 0, 4, 8, 14, and 18. The HVCs were dissected from each bird, and RT-PCR for VEGF was performed on the extracted HVC mRNA. Semiquantitative PCR revealed that HVC VEGF mRNA rose sharply within 4 days of testosterone treatment (Figure 2D). The normalized ratio of VEGF to G3PD mRNA was significantly higher on day 4 than at day 0 ($p < 0.01$ by two-way ANOVA), and it was stable for at least the 2 weeks thereafter. Thus, testosterone induced a burst of VEGF mRNA in HVC that preceded the onset of androgen-associated mitotic angiogenesis by 2–3 days.

The rise in VEGF mRNA was attended by a parallel increase in VEGF protein within HVC. ELISA revealed that in adult female canaries given silastic testosterone implants, HVC VEGF levels rose from 79.8 $\pm$ 15.4 ng VEGF/mg protein (4.8 $\pm$ 0.2 ng/g tissue) at baseline to 106.0 $\pm$ 10.8 ng/mg protein (8.3 $\pm$ 1.0 ng/g tissue) at 1 week after androgen treatment, and to 115.2 $\pm$ 21.2 ng/mg protein (7.7 $\pm$ 0.7 ng/g tissue) at 3 weeks. Two-way ANOVA revealed a highly significant overall effect of testosterone on HVC VEGF as a function of time ($p = 0.009$, $F = 5.63$ [2, 27 degrees of freedom {d.f.}]) (Figure 2E). No significant changes in VEGF were noted in the parahippocampus, archistriatum, or cerebellum of these birds (data not shown). In addition, immunocytochemistry revealed strong VEGF staining in the testosterone-treated HVC 6 days after testosterone treatment began (Figure 2C), whereas matched sections taken from cholesterol-treated control birds showed minimal VEGF-IR (data not shown).

VEGF Synthesis Was Selectively Localized to HVC

To localize VEGF-expressing cells in the testosterone-stimulated HVC, in situ hybridization was used to localize VEGF transcripts in birds given testosterone implants a week before sacrifice. VEGF cRNA probes were prepared based upon the PCR products generated from testosterone-treated canary brain mRNA that was reverse transcribed and subjected to PCR using rat VEGF primers. The resultant 406 bp canary VEGF fragment was sequenced and found to correspond to positions 122–526 of quail VEGF cDNA (96% homology) and to positions 166–404 of human VEGF 121/165 cDNA (82% homology). The canary VEGF partial cDNA was then cloned into pGEM (Promega) and transcribed into an RNA riboprobe using the T7 promoter. Using a P^{32}-labeled probe for in situ hybridization (ISH), we found that whereas the cholesterol-treated control canaries exhibited only low levels of VEGF mRNA expression throughout most of the caudal forebrain, their testosterone-treated counterparts exhibited significant VEGF mRNA in HVC. This androgen-induced VEGF mRNA was strikingly circumscribed to HVC, with relatively little expression elsewhere in the caudal forebrain, at least through the rostrocaudal extent subtended by HVC (Figures 2A and 2C). Control sections, which included testosterone-treated canary HVC probed with sense RNA as well as cholesterol-treated HVC probed with both sense and antisense RNAs, revealed little detectable forebrain VEGF mRNA by ISH and none in HVC.

VEGF, but Not the Gonadal Steroids, Was Mitogenic for HVC Endothelial Cells In Vitro

The testosterone-associated induction of endothelial cell proliferation in the adult HVC suggested either that the gonadal steroids—whether testosterone or its aromatized metabolite estradiol—were themselves mitogenic or that they acted to induce endothelial cell division through paracrine intermediaries such as VEGF. To

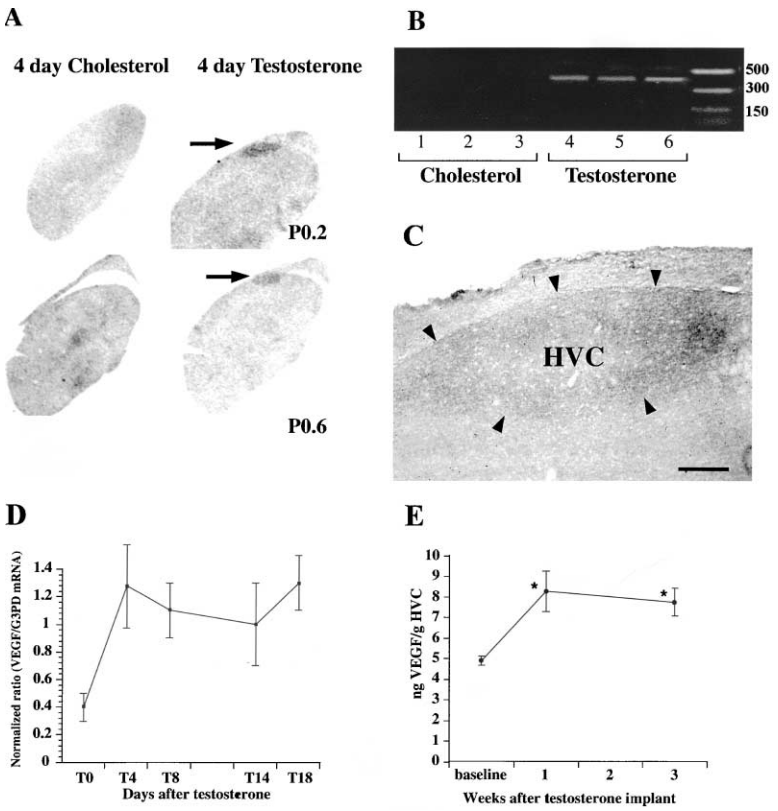

Figure 2. Testosterone Induces the Production of VEGF by the Adult HVC

(A) In situ hybridization using a P^{32}-labeled riboprobe revealed that VEGF mRNA was apparent in HVC within 4 days of testosterone silastic implantation. Within the area of the caudal forebrain studied, VEGF mRNA was sharply circumscribed to HVC.

(B) RT-PCR demonstrated the difference in VEGF mRNA between HVCs taken from three cholesterol and three testosterone-treated birds, all sacrificed 6 days after hormone implantation. The testosterone-associated VEGF surge was rapid in onset; HVC VEGF mRNA rose sharply within 4 days after testosterone implantation and peaked by 6–8 days.

(C) Immunolabeling revealed a distinct increase in HVC VEGF immunostaining within 6 days after testosterone treatment; at this time point, the increased VEGF immunoreactivity was locally restricted to HVC. Scale = 100 μm.

(D and E) Testosterone induced significant increases in HVC VEGF protein as well as mRNA. (D) This graph plots the normalized relative level of HVC VEGF mRNA as a function of time after testosterone implantation. These values were determined using semiquantitative PCR, with relative VEGF mRNA levels estimated at each time point as the normalized ratio of VEGF cDNA to G3PDH cDNA. By day 4, HVC VEGF mRNA was significantly more abundant than that at baseline ($p < 0.01$; see text). (E) This graph shows the parallel effect of testosterone on HVC VEGF protein, as measured by ELISA. The amount of VEGF in HVC, paralleling that of its mRNA, was significantly higher at 1 week than at baseline ($p < 0.01$).

assess whether the gonadal steroids might act directly as mitogens or whether they required paracrine intermediaries, we assessed their effects in cultures of canary neostriatal endothelia. These highly enriched endothelial cell cultures were prepared from the HVC and adjacent mediocaudal neostriata of adult canaries by fluorescence-activated cell sorting (FACS) of DiI-LDL-tagged dissociates of adult canary HVC (Leventhal et al., 1999). The resultant endothelial cultures were raised for 2 days in media containing 1% steroid-depleted FBS, and then they were exposed to testosterone (100 ng/ml), dihydrotestosterone (100 ng/ml), estradiol (10 ng/ml), cholesterol (100 ng/ml, as a negative control), BDNF (20 ng/ml), or VEGF (20 ng/ml, as a positive control), all in the presence of 3.5 μCi/ml [^{3}H]thymidine. The cultures were then extracted and net [^{3}H]thymidine incorporation counted by scintillation counter. We found that whereas VEGF was a strong mitogen for these cells, none of the gonadal steroids were (Figure 1D). Thus, whereas VEGF directly induces HVC endothelial cells to divide, the gonadal steroids are not directly mitogenic for these cells.

HVC Endothelia Upregulated VEGFR2/Quek1/KDR in Response to Gonadal Steroids

We next considered the possibility that gonadal steroids influenced not only VEGF production in HVC but also VEGF receptivity. The principal endothelial receptors for VEGF, the receptor tyrosine kinases VEGFR1/flt1 and VEGFR2/flk1/KDR, are both expressed minimally in unstimulated endothelium. We therefore asked whether HVC endothelial cells express VEGF receptors and whether VEGF receptor expression by these cells might be influenced by gonadal steroids. To this end, we assessed the expression of the principal known endothelial cell receptor for VEGF, VEGF-R2/Quek1, in hormone-treated female canaries in vivo as well as in isolated HVC endothelial cells in vitro.

Quek1 has been cloned from quail as the avian homolog of mouse flk-1 and human VEGF-R2/KDR, a VEGF receptor tyrosine kinase that is one of the two known high-affinity endothelial receptors for VEGF, the other being flt-1 (VEGF-R1) (Wilting et al., 1997). Lower affinity receptors for VEGF include the neuropilins, coreceptors for VEGF that are also expressed by neurons as their receptors for members of the semaphorin family of guidance molecules (Soker et al., 1998). Whereas VEGF-R1/flt1 and the neuropilins may be expressed by many cell types, VEGF-R2 is expressed by ECs, monocytes, and hematopoetic stem cells (Millauer et al., 1993); importantly, it may also be expressed by some neural populations in development (Yang and Cepko, 1996, Ogunshola et al., 2002). Given its restricted expression, we asked whether VEGF-R2/Quek1 was expressed by HVC ECs, and if so, whether its expression—like that of its ligand VEGF—might be modulated by testosterone.

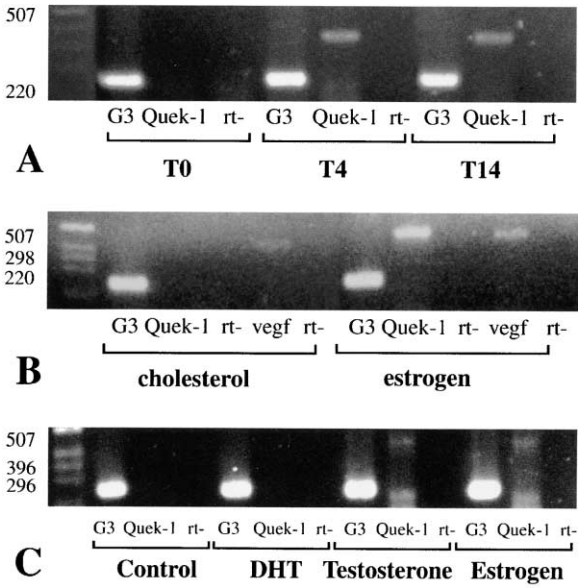

Figure 3. HVC Endothelial Cells Upregulate the VEGF-R2 Receptor, Quek1, in Response to Estrogen

(A) RT-PCR of mRNA isolated from adult female canary HVC (three birds pooled/time point) revealed that VEGF-R2/Quek1 mRNA rose sharply within 4 days of testosterone silastic implantation. Testosterone (T)0, T4, and T14 refer to the 0, 4, and 14 day timepoints after testosterone treatment.

(B) Treatment with estradiol yielded even more pronounced increases in Quek1 mRNA in the adult female canary HVC. This gel shows the RT-PCR products of mRNA derived from three pooled female HVCs 4 days after estradiol silastic implantation (right lanes) compared to cholesterol-treated control HVC (left). A small increase in VEGF signal was also noted in response to estradiol.

(C) Endothelial cells isolated from the mediocaudal neostriatum, which included HVC and the adjacent medial striatal wall, expressed Quek1 mRNA in response to estrogen stimulation in vitro. From left to right: reverse-transcribed Quek1 PCR products were not evident in endothelial cultures to which cholesterol (C) was added, but Quek1 signals were noted in both estradiol (E)- and testosterone (T)-supplemented media. No signal was evident in media supplemented with the nonaromatizable androgen 5α-dihydrotestosterone (DHT), suggesting that endothelial Quek1 was selectively induced by estrogen.

To amplify canary Quek1/VEGF-R2, we used quail-based primers to obtain a 405 bp fragment of canary Quek1. This corresponded to bases 2537–2941 of the quail Quek1 gene, with 89% homology to canary, and to bases 2519–2823 of human VEGFR2/KDR, to which canary Quek1 proved 83% homologous. We then assessed the effect of testosterone on Quek1/VEGFR2 mRNA by comparing Quek1 mRNA in testosterone-treated and control HVC (Figure 3A). Using RT-PCR, we found that Quek1 mRNA was scarcely detectable, if at all, in either the unstimulated or cholesterol-implanted adult female canary HVC. In contrast, within 4 days of testosterone treatment, HVC Quek1 levels rose substantially and remained high through day 14 (Figure 3A). Quek1 signal intensity slowly fell thereafter (data not shown), with a return to baseline level by 28 days.

Both Quek1 and VEGF Are Induced by Estradiol

The induction of endothelial VEGFR2/Quek1 by testosterone was dramatic and rapid. However, since testosterone may be aromatized to estradiol in the adult HVC, its actions may be mediated through either androgen or estrogen receptor systems. To distinguish which of these might be necessary for testosterone-induced VEGF-R2/Quek1 expression, we compared the effects of testosterone, estradiol-17β, and the nonnaromatizable androgen 5-α-dihydrotestosterone (DHT) on Quek1 expression by isolated HVC endothelial cells in vitro. We found that Quek1 mRNA was induced in cultured canary neostriatal endothelial cells within 2 days of testosterone exposure; these cells expressed no detectable Quek1 mRNA in the absence of gonadal steroid treatment. This effect appeared specifically mediated by estrogen, in that estradiol-17β induced endothelial Quek1/VEGFR2 whereas the purely androgenic 5α-DHT did not (Figure 3C).

We have previously noted that estradiol, like testosterone, is associated with endothelial cell division in the adult canary HVC, although the endothelial mitotic index achieved is less than that yielded by androgen treatment (Hidalgo et al., 1995). On this basis, we asked whether estrogen might induce Quek1 in vivo, just as in vitro, thereby allowing ambient VEGF to activate local endothelial cells. We treated six adult females with silastic implants containing either estradiol-17β or cholesterol ($n = 3$ birds each) and sacrificed them at various time points thereafter, subjecting their dissected HVCs to RT-PCR for the Quek1/VEGFR2 receptor as well as for VEGF itself. We found that estradiol induced HVC Quek1/VEGFR2 within 4 days of treatment (Figure 3B). Furthermore, VEGF mRNA also rose in response to estradiol, roughly following the same time course as Quek1/VEGFR2 (data not shown). The importance of estradiol in the induction of VEGF is also suggested by the finding that the VEGF promoter harbors an estrogen response element that binds estradiol-estrogen receptor complexes and is able to direct VEGF transcription (Mueller et al., 2000). Together, these observations suggest that estrogen may be a critical intermediary in the stimulation of HVC angiogenesis by testosterone.

The Adult Female HVC Produces BDNF mRNA and Protein in Response to Testosterone

BDNF expression in the canary HVC is sexually dimorphic, being higher in the adult male than the female, and testosterone treatment has been shown to induce BDNF in the adult female HVC (Rasika et al., 1999). To better understand the role of androgen-induced BDNF in HVC neuronal recruitment, as well as its potential relationship to androgen-associated angiogenesis, we sought to define the time course of testosterone-induced BDNF expression. Using RT-PCR, in situ hybridization, and ELISA, we found that HVC BDNF mRNA and protein both rose significantly in response to testosterone, though according to a notably delayed time course.

By PCR and ISH, BDNF mRNA levels in HVC appeared to rise only after a delay of at least 2 weeks following initial testosterone treatment. Semiquantitative RT-PCR normalized against G3PD mRNA revealed no detectable elevation in BDNF mRNA at 4 or 8 days after testosterone treatment, but did detect a substantial increase in BDNF signal by 14 and 18 days (Figure 4A). ELISA revealed that BDNF protein levels remained roughly stable for at

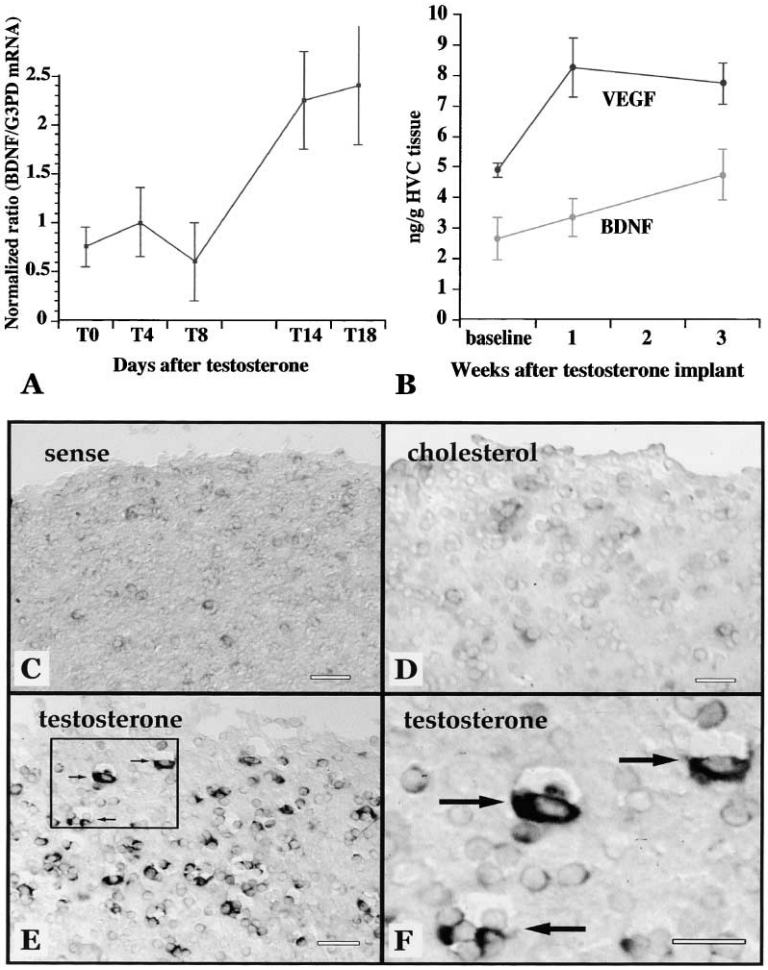

Figure 4. Testosterone Induces the Production of BDNF in Both HVC and Its Endothelial Cells

(A) RT-PCR revealed a sharp but delayed rise in HVC BDNF mRNA after testosterone treatment. This rise in BDNF mRNA was first manifest, and achieved statistical significance (see text), 14 days after silastic implantation.

(B) ELISA similarly revealed that the concentration of HVC BDNF protein changed little in the first week after testosterone, but rose steadily thereafter. The delayed rise in BDNF contrasted with the rapid elevation in HVC VEGF (superimposed from Figure 2), which achieved its maximum within a week of androgen treatment. Like the level of BDNF mRNA, the concentration of BDNF protein at 3 weeks was significantly higher than that measured either at baseline or at 1 week; the latter two values did not statistically differ (see text).

(C–F) In situ hybridization for BDNF cRNA in canaries treated with testosterone 18 days prior to sacrifice compared to cholesterol-treated controls. (C) A control section probed with BDNF sense cRNA; (D) HVC of cholesterol-treated controls revealed a low level of baseline BDNF mRNA expression, which was predominantly neuronal. (E and F) Sections probed with BDNF antisense cRNA revealed a marked increase in BDNF signal in the testosterone-treated HVC at 18 days. (F) A higher magnification view shows that much of the increment in BDNF mRNA was perivascular and associated with capillary endothelial cells (arrows). Scale = 30 μm.

least the first week after testosterone treatment, measuring 40.3 ± 9.4 μg BDNF/g protein (2.62 ± 0.7 ng/g tissue) on the day of testosterone implantation, and 41.7 ± 4.0 μg/g (3.3 ± 0.6 ng/g tissue) at 7 days. Thereafter, the concentration of HVC BDNF rose to achieve a level of 70.2 ± 23.2 μg/g (4.7 ± 0.8 ng/g tissue) by 3 weeks after testosterone treatment. Thus, within 3 weeks after testosterone implantation, HVC BDNF levels rose by 79% (when expressed in μg/g protein, or by 74% when expressed in ng/g tissue) (Figure 4B). The relatively delayed accumulation of BDNF in the testosterone-treated HVC contrasted sharply with the rapid elevation in HVC VEGF and VEGF-R2/Quek1, each of which rose significantly in the first week after androgen treatment (Figures 2 and 3).

ISH revealed that BDNF cDNA exhibited a substantial elevation in signal intensity in the HVCs of testosterone-treated birds. The elevation in BDNF's hybridization signal was first noted 14 days after androgen administration. By 17 days after testosterone treatment—a time point chosen on the basis of the PCR data—ISH revealed a marked increase in BDNF mRNA expression in HVC in the testosterone-treated animals (Figure 4C). The cellular basis for this increased BDNF mRNA signal proved surprising; HVC BDNF mRNA was associated with both morphologically-evident neurons and satellite astrocytes, as previously reported (Dittrich et al., 1999; Li et al., 2000). However, the testosterone-treated birds were also specifically distinguished by prominent BDNF mRNA expression by HVC microvascular capillary cells. In contrast, the control birds exhibited little or no such perivascular BDNF mRNA. Thus, testosterone treatment was associated with a marked, but relatively delayed upregulation of BDNF in HVC. Importantly, the capillary microvasculature contributed substantially to that increment.

Purified Cultures of HVC Endothelial Cells Synthesize and Secrete BDNF

We have previously noted that capillary endothelial cells secrete BDNF protein and that they may do so in sufficient amounts to support the migration and survival of neurons arising from the adult rat ventricular zone (Leventhal et al., 1999). To assess whether androgen-induced angiogenesis might contribute to neuronal recruitment in HVC through endothelial-derived BDNF, we investigated the release of neurotrophins by microvascular ECs derived from the adult HVC. These ECs were harvested by FACS of DiI-LDL-tagged dissociates of adult canary HVC and adjacent mediocaudal neostriatum, as previously described (Leventhal et al., 1999). When raised in base media supplemented only with 2% steroid-depleted FBS and hydrocortisone, the cells expressed measurable levels of both BDNF mRNA and

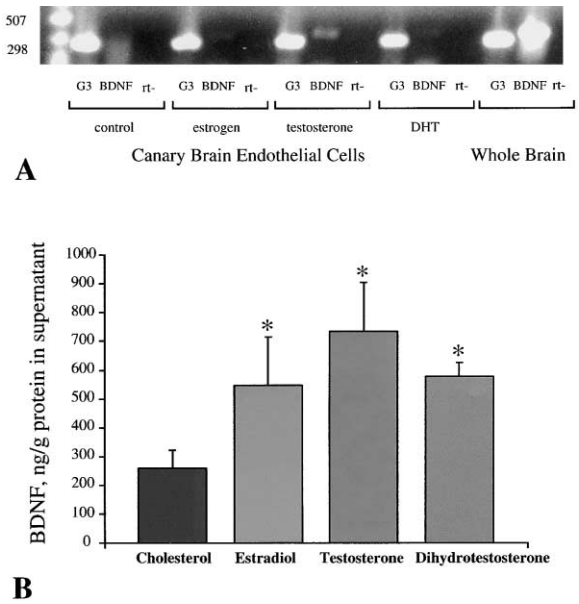

Figure 5. Cultured HVC Endothelial Cells Exhibit Gonadal Steroid-Dependent BDNF Production

(A) RT-PCR revealed that HVC/MCN endothelial cells, harvested by FACS of DiI-LDL-tagged dissociates of the adult canary mediocaudal neostriatum, synthesized BDNF; this process was stimulated by testosterone, and less so by estradiol and DHT.

(B) ELISA confirmed that BDNF was secreted by the endothelial cells and that this too was strongly promoted by testosterone, the addition of which more than tripled the rate of BDNF release from these adult neostriatal endothelial cells. Asterisks denote statistically higher levels of BDNF release than those of cholesterol-treated controls ($p < 0.05$; see text).

protein (Figure 5). ELISA revealed that after 2 days in vitro, these HVC ECs released a baseline level of 258 ± 62 ng BDNF/g into the culture supernatant. This level of endothelial BDNF secretion approximated that which we previously noted in unstimulated cultures of human brain microvascular endothelial cells (Leventhal et al., 1999). These observations suggested that the capillary vasculature of the adult songbird HVC can serve as a local secretory source of BDNF.

Testosterone and Estrogen Induce BDNF Production by Cultured HVC Endothelial Cells

On the basis of the twin observations that gonadal steroids can induce BDNF production and that HVC ECs might themselves serve as important sources of BDNF, we next asked whether neostriatal capillary ECs modify their levels of BDNF secretion in response to gonadal steroid activation. To this end, plates of FACS-purified neostriatal endothelial cells were raised in serum-free media supplemented with VEGF alone for 2 days, and then were exposed to estradiol, testosterone, 5α-DHT, or cholesterol for 48 hr ending at the end of day 4 in vitro. At that point, matched cultures were extracted for either protein for BDNF ELISA or mRNA for semiquantitative PCR.

We found that testosterone predictably elevated the level of BDNF mRNA expressed by these endothelial layers (Figure 5A). This contrasted with matched cholesterol-treated controls, which exhibited scarcely detectable BDNF message, and with estradiol- and 5α-DHT-exposed cultures, which showed lesser though consistent elevations in BDNF mRNA. Similarly, ELISA of endothelial culture supernatants revealed that the concentration of BDNF protein in testosterone-treated cultures, 69.8 ± 27 pg/ml (733 ± 173 ng/g protein), was significantly higher than in matched cholesterol-treated controls, which had 23.8 ± 4.4 pg BDNF/ml (258.3 ± 62.2 ng/g) ($p = 0.025$; $F = 8.84$ [1, 6 d.f.]). Both estradiol- and 5α-DHT-exposed cultures exhibited lesser elevations in BDNF protein; estradiol-treated endothelial cultures harbored 46.5 ± 9.4 pg BDNF/ml (546 ± 169 ng/g), and DHT-treated plates had 41.4 ± 8.4 pg/ml (576 ± 349 ng/g) (Figure 5B). Together, these findings indicated that gonadal steroids directly induced BDNF transcription and release by neostriatal endothelial cells.

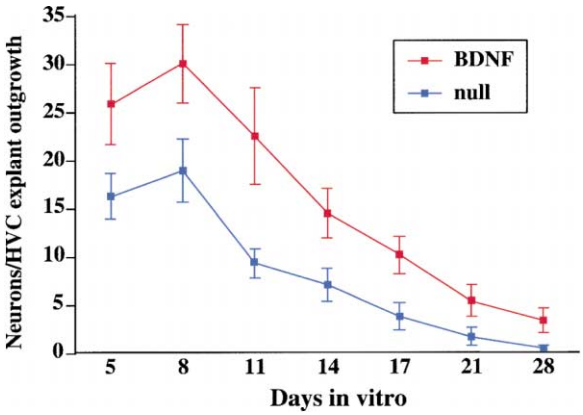

Figure 6. BDNF Promotes Neuronal Outgrowth from the Cultured Adult HVC VZ

This graph plots the number of neurons observed in the outgrowths from adult HVC VZ explants, either BDNF-supplemented or not, as a function of time in vitro. BDNF (20 ng/ml) was noted to significantly increase both the numbers of neurons departing these explants and their relative abundance thereafter through the first 24 days in vitro ($p < 0.001$; see text).

BDNF Promotes the Migration and Recruitment of Neurons from the HVC Ventricular Zone In Vitro

To establish whether the appearance of neurons arising from the adult HVC ventricular zone (VZ) was directly supported by BDNF, we assessed the outgrowth of neurons from explants of adult canary HVC. To this end, five adult female canaries were sacrificed for HVC VZ explant culture, as described (Goldman et al., 1992). These were raised in either base medium (DMEM/F12/N2 with 10% platelet-depleted FBS) or the same supplemented with 20 ng/ml BDNF. Neurons arising from the explants were scored using established morphological criteria (Goldman, 1990; Kirschenbaum and Goldman, 1995) and counted twice weekly for 3 weeks thereafter (seven timepoints). We found that the number of neurons arising from these explants was significantly higher in BDNF-supplemented plates than in unsupplemented controls ($p < 0.001$; $F = 31.5$ [1, 6 d.f.]) (Figure 6). BDNF's support of neuronal differentiation and migration from

these adult HVC explants was compatible with its role in promoting the recruitment of new neuronal migrants in vivo (Rasika et al., 1999; Zigova et al., 1998).

VEGF Signaling Is Necessary for Testosterone-Induced Angiogenesis

On the basis of the temporal and spatial associations between BDNF production by the testosterone-stimulated HVC microvasculature and neuronal recruitment, we asked whether endothelial cell proliferation was *necessary* for testosterone-dependent neuronal recruitment. To this end, we first assessed the effect of inhibiting VEGF-R2 signaling upon testosterone-induced HVC endothelial cell division, using a small molecule inhibitor of the VEGF-R2/KDR tyrosine kinase, 4-[(4′-chloro-2′-fluoro)phenylamino]-6,7-dimethoxy-quinazoline (Calbiochem 676475). We chose this agent, which we will designate VEGFR-TKI (VEGF receptor tyrosine kinase inhibitor), for several reasons. First, it is highly potent (IC_{50} = 0.1 μM for VEGF-R2/KDR/flk1/Quek1 and 2 μM for VEGF-R1/flt1), yet is more specific for VEGF-R2 than other currently available inhibitors of the KDR tyrosine kinase, with <1% cross-inhibition of the PDGF, HGF, or FGF2 receptors (Hennequin et al., 1999). Second, VEGFR-TKI is small, has a low hydrogen bond number, and is highly lipophilic, permitting ready penetration of the blood-brain barrier (Pardridge, 1995). Third, in both experimental and clinical trials, its similar but less blood-brain barrier-permeable analog ZD4190 has shown little or no systemic toxicity at doses an order of magnitude higher than those employed here (Wedge et al., 2000).

To determine the effect of inhibiting VEGF signaling on HVC angiogenesis, we thus injected six testosterone-treated canaries with either VEGFR-TKI (2.5 mg/kg, or typically, 50 μg/20 g bird) or vehicle (DMSO:PBS, 2:1) for 9 days, starting on the day of steroid implantation (n = 3 each). Throughout the experiment, the birds were also injected twice daily with bromodeoxyuridine (BrdU; 50 mg/kg intrapectoral q12 hr) to label newly generated cells. The canaries were sacrificed on day 10, and their brains were removed, cryosectioned, and double-immunolabeled for BrdU and laminin. For each HVC, the incidence of laminin$^+$/BrdU$^+$ cells and the ratio of laminin$^+$/BrdU$^+$ cells to total HVC laminin$^+$ ECs were determined bilaterally in each of five sections spaced 100 μm apart. For total endothelial counts, individual ECs were defined by double-labeling with the nuclear dye DAPI and laminin. Using this protocol, we found that testosterone-treated birds injected with vehicle control had an HVC endothelial labeling index of 4.89% ± 0.6% (221 BrdU$^+$/laminin$^+$ cells among a total of 4536 laminin$^+$/DAPI$^+$ cells). Strikingly, the endothelial labeling index of testosterone-treated birds injected with VEGFR-TKI fell by over 60%, to 1.94% ± 0.4%, (66 BrdU$^+$/laminin$^+$ cells among 3403 laminin$^+$/DAPI$^+$ cells). Thus, pharmacological inhibition of VEGF signaling substantially reduced testosterone-mediated HVC angiogenesis ($p = 0.002$ by one-way ANOVA; $F = 47.9$ [1, 4 d.f.]).

VEGF Signaling Is Necessary for Testosterone-Induced Neuronal Recruitment

We next sought to determine if the inhibition of HVC endothelial proliferation would reduce neuronal recruitment to HVC. Sixteen 1-year-old female canaries were injected twice daily with bromodeoxyuridine (BrdU; 50 mg/kg intrapectoral q12 hr) for 7 days beginning with day 1 in order to label newly generated cells. On day 8, they were all implanted with either testosterone-containing or empty (control) silastic implants. Beginning on day 8, the canaries were also injected twice daily with either VEGFR-TKI (2.5 mg/kg, or typically, 50 μg/20 g bird) or a vehicle control (DMSO:PBS, 2:1). In this way, the 16 canaries were grouped into four treatment categories (n = 4 birds/group): (1) no hormone/vehicle; (2) no hormone/VEGFR-TKI; (3) testosterone/vehicle; and (4) testosterone/VEGFR-TKI. Treatment with VEGFR-TKI was continued from days 8–33, and the canaries were sacrificed on day 40. Their brains were removed, sectioned at 14 μm, and double-stained for BrdU and Hu, a neuron-specific RNA binding protein that is uniformly and selectively expressed by neurons within the adult HVC (Barami et al., 1995). For each of the 16 birds, the ratio of Hu$^+$/BrdU$^+$ cells to the total number of Hu$^+$ neurons within each cresyl violet-defined HVC was determined bilaterally in each of five sections spaced 100 μm apart. These were chosen to span the stereotaxic coordinates AP0.0-P0.5 (Stokes et al., 1976), a region that includes most of the volume of the adult HVC.

Using this protocol, we found that the mitotic index of Hu$^+$ HVC neurons in testosterone-treated birds not injected with inhibitor was 1.91% ± 0.1%. This included 647 BrdU$^+$/Hu$^+$ cells among a total of 33,766 Hu$^+$ neurons in 40 scored sections. This incidence was 3.4-fold greater than the 0.56% ± 0.1% neuronal labeling index (188 BrdU$^+$/Hu$^+$ cells among 33,666 Hu$^+$ cells) found in control birds given no inhibitor and an empty silastic (Figure 7). This effect of testosterone on the neuronal labeling index was highly significant when assessed by two-way ANOVA ($F = 382.9$ [1, 1, 15 d.f.]; $p < 0.0001$), confirming that testosterone promotes the recruitment of new neurons to the HVCs of adult female canaries. However, when a matched cohort of testosterone-treated females was injected with VEGFR-TKI, the testosterone-induced increase in the Hu$^+$ neuronal labeling index was suppressed by 46%, to 1.04% ± 0.1% (337 BrdU$^+$/Hu$^+$ cells among a total of 32,451 neurons). When assessed by ANOVA, this reduction in the labeling index was highly significant ($F = 163.9$; $p < 0.01$ after post hoc Boneferroni correction). The marked suppression of the Hu$^+$/BrdU$^+$ neuronal labeling index by the VEGFR tyrosine kinase inhibitor demonstrated that VEGF signaling was indeed required for testosterone-dependent neuronal recruitment to HVC.

To determine whether VEGFR-TKI influenced baseline levels of neuronal recruitment, canaries not treated with testosterone were also injected with the inhibitor. The resulting labeling index of Hu$^+$ neurons in these inhibitor-treated hormonal nulls was 0.51% ± 0.02%, not significantly different than the 0.56 ± 0.01% labeling index found in birds given empty silastics and no inhibitor ($F = 0.37$, $p > 0.05$) (Figure 7).

Discussion

In this study, we asked whether testosterone-induced endothelial cell proliferation in the adult canary vocal control nucleus HVC might be causally related to the

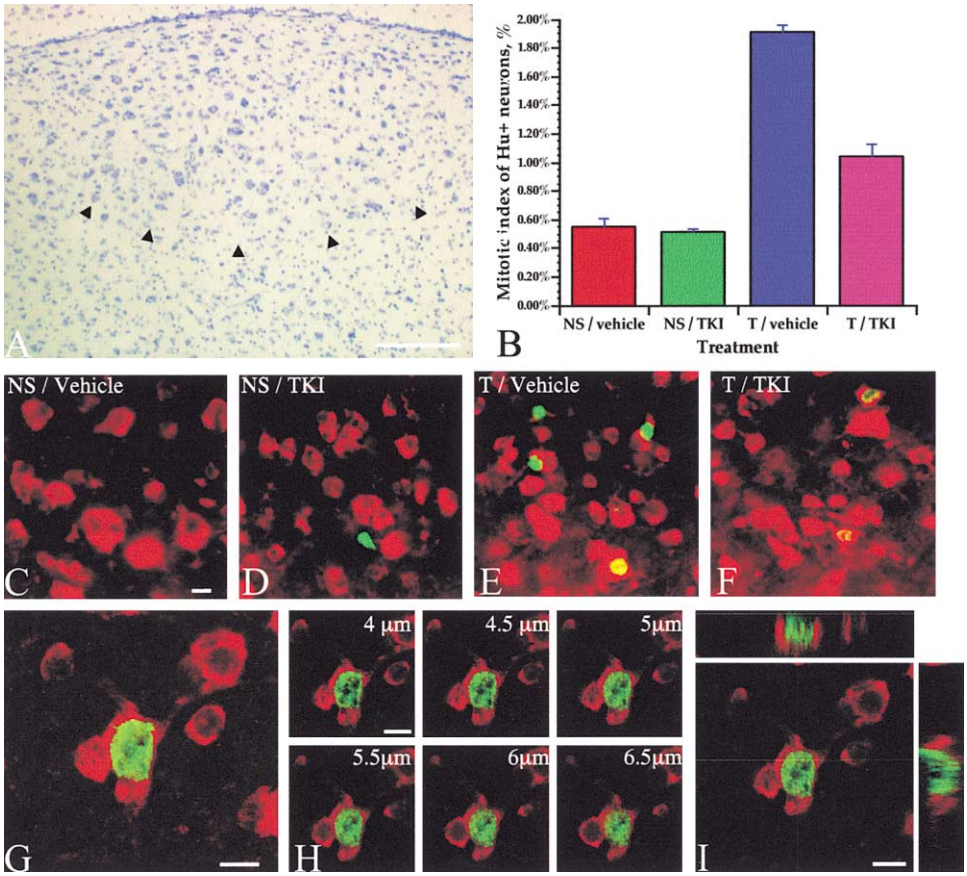

Figure 7. Inhibition of VEGF Signaling Suppresses Testosterone-Induced Neuronal Recruitment

(A) This section shows the borders of a cresyl violet-stained HVC 1 month after administration of a testosterone silastic. Arrowheads identify the border of HVC, delimiting the region scored.

(B) This plot compares the number of newly recruited $BrdU^+/Hu^+$ neurons, expressed as a percentage of all Hu^+ HVC neurons, between birds in four treatment groups. These include both testosterone-treated (T) and untreated (NS: null silastic) birds given either a VEGF-R2/Quek1/KDR tyrosine kinase inhibitor (VEGF-TKI) or a DMSO vehicle control (vehicle). VEGF TK inhibition was associated with an almost 50% reduction in the number of $BrdU^+/Hu^+$ neurons recruited to HVC over the month after androgen administration.

(C–F) Examples of $BrdU^+/Hu^+$ neurons in each of these groups: (C) an empty silastic null control subsequently injected only with vehicle (NS/vehicle); (D) an empty silastic NS control given the VEGF tyrosine kinase inhibitor (NS/TKI); (E) a testosterone-treated bird otherwise given only vehicle, as a positive control (T/vehicle); (F) a testosterone-treated bird given VEGFR TKI (T/TKI).

(G–I) Confocal validation of the double-labeling of a $BrdU^+$ (green)/Hu^+ (red) neuron noted in the HVC of a testosterone-implanted adult female 1 month after hormone administration. (G) A composite z stack of a series of six confocal images taken 0.5 μm apart (H), and (I) as viewed orthogonally in the *xz* and *yz* planes. Scale: (A), 100 μm; (C–I), 10 μm.

induction and success of adult neurogenesis therein. We found the following. (1) Testosterone treatment resulted in the production of vascular endothelial growth factor, VEGF, within the adult HVC. (2) The resultant VEGF surge was spatially localized to HVC, within which it was temporally associated with the proliferation of capillary endothelial cells. This led to an expansion of the microvasculature within, but not beyond, HVC. (3) ECs purified from the adult canary HVC responded to testosterone and estradiol by upregulating their expression of the VEGF receptor, VEGF-R2/Quek1. This in turn enabled the cells to proliferate in response to VEGF. (4) Both BDNF mRNA and protein levels rose substantially in HVC after testosterone treatment, with a time course that followed, by over a week, testosterone's induction of VEGF and its receptor. (5) HVC ECs synthesized and secreted the neurotrophin BDNF, suggesting that the VEGF-expanded vasculature increased BDNF availability within the HVC. (6) The production of BDNF by HVC ECs could be modulated by gonadal steroids. Steroid-induced endothelial BDNF production appeared largely androgenic, in that both testosterone and DHT yielded substantial increments in endothelial BDNF mRNA and protein. (7) BDNF supported the emigration of neurons from explants of the adult HVC ventricular zone, suggesting that BDNF directly promotes neuronal recruitment into the HVC parenchyma. (8) Both testosterone-induced angiogenesis and neuronal addition to the adult HVC could be substantially diminished by inhibition of VEGF tyrosine kinase activity. Together, these findings suggest a causal interaction of testosterone-induced angiogenesis and neurogenesis in the adult songbird brain (Figure 8).

The Source and Role of Androgen-Stimulated VEGF

The induction of VEGF appeared to be an early and cardinal event in the sequence of events leading to androgen-associated neuronal recruitment to HVC. Cer-

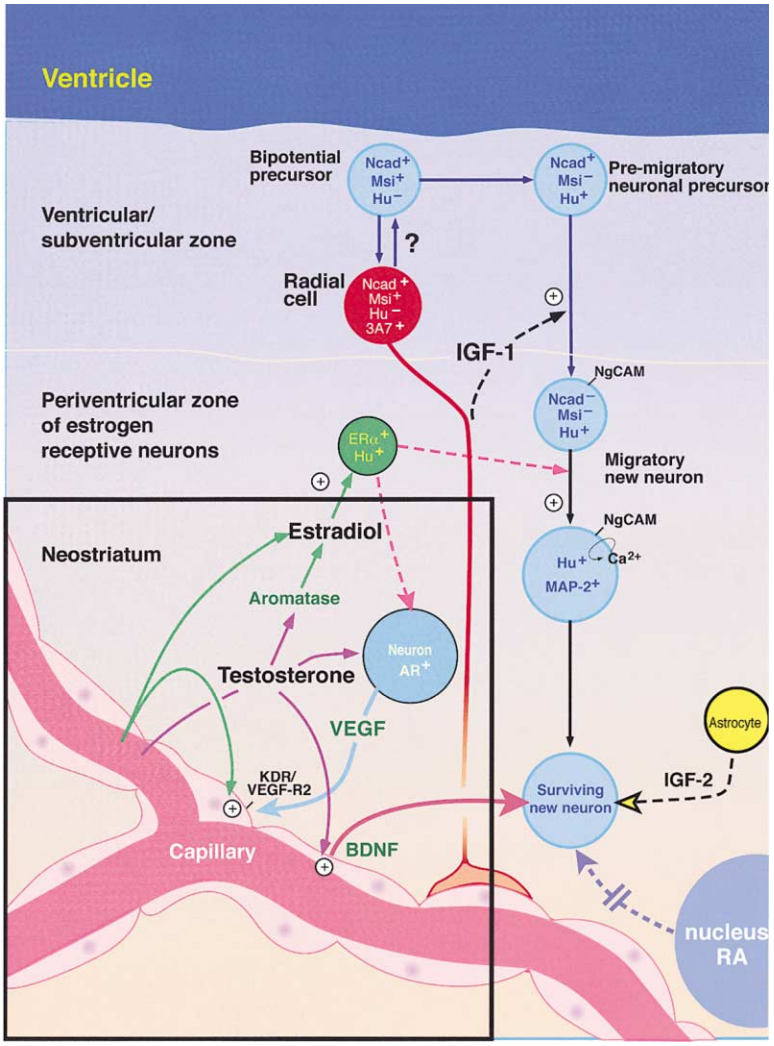

Figure 8. Our Model: An Orchestrated Series of Paracrine Interactions Permits Neuronal Recruitment

This schematic summarizes our understanding of the means by which the gonadal steroids may influence neuronal recruitment to the adult HVC. The boxed-in area surrounding the capillary at the lower left highlights the role of testosterone-associated angiogenesis in this process. These pathways are presented in the context of complementary recent findings pertaining to the cellular basis for neuronal recruitment in the adult HVC (Barami et al., 1994, 1995; Bottjer and Johnson, 1997; Holzenberger et al., 1997; Jiang et al., 1998; Goldman, 1998; Goldman and Luskin, 1998).

Abbreviations: Ncad, N-cadherin; AR, androgen receptor; ER, estrogen receptor-α; IGF-1, insulin-like growth factor-1; Hu, Hu protein; 3A7, a vimentin-associated antigen; VEGF, vascular endothelial growth factor; Quek1, the VEGF receptor VEGF-R2/Quek1/KDR; BDNF, brain-derived neurotrophic factor.

tainly, the testosterone-associated increment in HVC VEGF protein from 79.8 ± 15.4 to 115.2 ± 21.2 μg/g, occurring concurrently with a sharp upregulation in VEGF mRNA as measured by both PCR and ISH, argued that androgen-induced angiogenesis was based upon the antecedent induction of VEGF synthesis in HVC. Yet it may be instructive to note that even though no such VEGF mRNA was detected within the unstimulated HVC, either by RT-PCR or ISH, the unstimulated HVC nonetheless still harbored an average of almost 80 μg VEGF/g protein. This suggested that some VEGF protein may reside within HVC as a relatively stable pool, perhaps matrix bound. This is of interest given recent observations that proteolytic matrix metalloproteinases (MMPs), and MMP-9 in particular, may activate angiogenesis by releasing resident VEGF from stores bound within the interstitial matrix (Bergers et al., 2000). This suggested the possibility of a similar, androgen-evoked proteolytic liberation of VEGF from tissue stores sequestered within the quiescent adult HVC. Together, these observations suggest that while androgen-induced HVC angiogenesis is causally preceded by the local synthesis of VEGF, other, transcriptionally independent mechanisms, such as the androgen-elicited release of tissue-bound VEGF, may also cooperate to induce angiogenesis.

VEGF May Act to Induce Local Vascular Permeability

VEGF mobilized from the HVC interstitial matrix, as well as that produced locally thereafter, might mediate not only angiogenesis, but also local increases in local vascular permeability (Nag et al., 1997; Proescholdt et al., 1999; Yancopoulos et al., 2000; Zhang et al., 2000). Among other effects, such focal vasogenic edema might increase the access of systemically bound agents to the testosterone-treated HVC. As such, one cannot rule out the possibility that markers of DNA replication and mitosis, such as bromodeoxyuridine and labeled thymidine, might enjoy preferential access to HVC in testosterone-stimulated birds. To be sure, we have found no evidence for such effects in these studies, and VEGF clearly induced endothelial cell mitotic labeling in vitro as well as in vivo. In addition, BrdU in particular has wide availability to normal brain tissue following systemic administration and does not require tissue disruption for cerebral parenchymal access. Nonetheless, the androgen-induced vascular permeability that may be associated with angiogenic regions as such as HVC might serve as an important example of hormonal regulation of blood-brain barrier permeability in the adult brain. Indeed, future studies may prove the HVC a unique model

for reversible hormonal disruption of the normal adult blood-brain barrier.

Potential Collaborative Angiogenic Agents

It is important to note that whereas VEGF mRNA and protein both remained elevated after testosterone silastic implantation, mitotic angiogenesis in the testosterone-treated adult HVC is relatively short-lived. The endothelial mitotic indices of the androgen-stimulated HVC fall within 2 weeks of the initial burst of hormone-induced angiogenesis (Goldman and Nottebohm, 1983). Thus, androgen-associated angiogenesis appears to follow a parabolic time course, despite the persistent elevation of HVC VEGF. Rather than representing local endothelial tachyphlaxis to VEGF, it is likely that VEGF's role changes during persistent endothelial activation from inducing mitogenesis to supporting capillary maintenance (Hanahan, 1997). This may be a function of other angiogenic factors released in the androgen-stimulated tissue (Suri et al., 1996). The latter possibility is suggested by the observation that VEGF's actions may shift from inducing endothelial division to supporting vascular modeling once the new endothelial cells are stimulated by angiopoetin-1 (Suri et al., 1998; Thurston et al., 1999). The latter is serially activated during angiogenesis and may induce endothelial cells to recruit smooth muscle pericytes to the nascent capillary wall (Yancopoulos et al., 2000). Thus, VEGF's actions may vary as a function of the local coexpression of other angiogenic growth factors released in the androgen-stimulated HVC, whether in parallel with or downstream to VEGF.

Sequential Activation of VEGF-R2/Quek1, VEGF, and BDNF in the Testosterone-Stimulated HVC

Our results suggest that gonadal steroid-modulated angiogenesis in HVC depends not only upon the release of VEGF by androgen-receptive cells in the region, but also on the concurrent induction of the endothelial receptor for VEGF. Previous studies have found that both neurons and astrocytes express androgen receptor mRNA (Nastiuk and Clayton, 1995); either of these cell types might be potential sources of testosterone-associated VEGF. In HVC, the transcriptional activation and synthesis of VEGF after testosterone exposure was swift; within 4 days of silastic implantation, HVC VEGF rose to levels readily detectable by RT-PCR, immunolabeling, and ELISA. Moreover, testosterone's induction of VEGF's endothelial receptor, VEGF-R2/Quek1, was similarly rapid and even more marked in degree; within 2–4 days of androgen exposure, a sharp upregulation in Quek1 mRNA was observed in both HVC tissue and isolated endothelial cells. Indeed, VEGF-R2/Quek1's relative absence in the unstimulated HVC, its rapid expression in response to testosterone, its importance to VEGF-activated vascular expansion, and the importance of the latter in BDNF release suggested that the induction of the VEGF receptor might represent a critical checkpoint in the process of testosterone-modulated neuronal recruitment.

Androgens and Estrogens Collaborate to Induce HVC Angiogenesis

The induction by testosterone of VEGF-R2/Quek1 in HVC was reproduced in neostriatal ECs in vitro, in which testosterone induced an increase in endothelial VEGF-R2 mRNA within 48 hr. Importantly, dihydrotestosterone elicited no such induction of VEGF-R2/Quek1, even though DHT did elicit BDNF production in matched cultures of neostriatal endothelial cells. Thus, the induction of Quek1 receptor by gonadal steroids appeared to be mediated by estrogen rather than androgen receptor-dependent pathways. A role for this pathway is also suggested by the high level of aromatase, which converts testosterone to estradiol, in the mediocaudal neostriatum of adult songbirds (Balthazart et al., 1996; Shen et al., 1995) and by the regulation of aromatase expression by testosterone (Fusani et al., 2001). A direct estrogenic induction of endothelial VEGF-R2/Quek1 is particularly attractive in light of the widespread vascular expression of both the ERα and ERβ families of estrogen receptors (Iafrati et al., 1997; Lindner et al., 1998; Mosselman et al., 1996). ERα is expressed heavily in HVC (Bernard et al., 1999; Gahr, 1990) and may modulate both the endothelial expression of, and response to, humoral cytokines (Caulin-Glaser et al., 1996). ERβ is expressed by both vascular endothelial and smooth muscle cells in mammals (Andersson et al., 2001) and is a potential mediator of the estrogenic induction of Quek1, although recent studies have not identified ERβ in HVC (Bernard et al., 1999). Pending further study of the phenotypic specificities and regulation of these receptors in the canary HVC, each remains a candidate to mediate the effects of gonadal steroids on endothelial production of neuronal cytokines. Such vascular estrogen receptors might thereby prove important to the genesis of sexually dimorphic neural architecture and behaviors alike.

The induction of endothelial KDR/Quek1 by gonadal steroids appears to be rate limiting for VEGF's activation of ECs in the adult HVC. This process appears likely to be triggered by circulating testosterone acting through an estrogenic intermediary, presumably after its in situ aromatization to estradiol. Together, these results indicate that testosterone stimulates angiogenesis in the adult HVC by concurrently inducing the expression of VEGF and its principal receptor VEGF-R2/Quek1 in neural and endothelial cells, respectively. This in turn suggests a tight coordination of androgenic and estrogenic actions in mediating steroid-induced angiogenesis in the adult songbird brain.

BDNF and the Direction of Neuronal Recruitment to the Testosterone-Stimulated HVC

Our results indicate that the testosterone-stimulated HVC vascular bed may constitute a major local source of BDNF. The effects of this regional burst in tissue BDNF on HVC neurogenesis are likely manifold; besides its actions as a survival factor for neurons generated in adulthood (Kirschenbaum and Goldman, 1995; Rasika et al., 1999; Zigova et al., 1998), BDNF has been shown to be a chemotactic cytokine for fetal neurons in tissue culture (Behar et al., 1997). As such, HVC BDNF may act as a chemotactic factor for newly migratory neurons upon their departure from the VZ. This is particularly intriguing since dividing endothelial cells of the testosterone-stimulated adult HVC are spatially delimited to HVC, and the highest density of new neurons added to

the androgen-treated mediocaudal neostriatum is within HVC (Alvarez-Buylla and Nottebohm, 1988). Together, these observations suggest that the HVC microvasculature, by secreting BDNF into the local parenchyma, might establish a vectorial gradient of BDNF sufficient to attract neuronal migrants to sites of endothelial cell activation, including those of active or recent angiogenesis. As such, endothelial BDNF might serve as both a chemoattractant and humoral neurotrophin for neuronal migrants departing the VZ, directing them to the HVC capillary bed, wherein they may integrate and survive under the influence of the high local concentrations of BDNF.

Gonadal Steroids Act at Several Levels to Regulate HVC BDNF

Our observations suggest that two serially activated pathways collaborate to provide a permissive environment for gonadal steroid-induced endothelial BDNF production. First, gonadal steroid-induced endothelial VEGF-R2/Quek1 expression sensitizes the capillary bed to respond to VEGF. Next, testosterone-induced VEGF, generated as a paracrine angiogenic factor by androgen-receptive cells in HVC, activates Quek1 to stimulate local HVC angiogenesis. The remodeled vessels then express BDNF, and they do so in an androgen-dependent manner. As a result, the androgen-induced expansion of the HVC capillary vasculature is followed, roughly 2 weeks later, with a geographically discrete upregulation of BDNF mRNA and protein. The rise in HVC BDNF is thus a function of both the expanded vascular bed in HVC and the gonadal steroid-enhanced production of BDNF by the cells therein.

The Importance of Endothelial BDNF

The increased endothelial expression of BDNF mRNA in the testosterone-stimulated birds, coupled with the robust secretion of BDNF by HVC ECs in vitro, suggested that the capillary endothelium might be a major contributor to total BDNF in the testosterone-stimulated adult canary HVC. This in turn suggests that ECs might be a major source of BDNF-associated neurotropism in this system. In a recent study of adult-derived human brain endothelial cells (HBECs), we noted that cultured HBECs secreted $>$1 ng BDNF/10^6 cells/24 hr (Leventhal et al., 1999). In the present study, we similarly found that canary brain ECs secreted an average of 1 ng BDNF/10^6 cells/24 hr under our culture conditions. These concentrations are more than sufficient to promote and support neuronal migration and survival (Leventhal et al., 1999).

The functional importance of this endothelial contribution to the total testosterone-associated increment in HVC BDNF is suggested by the observation that HVC BDNF levels first rose during the third week after testosterone administration, only after the expansion and stabilization of the HVC capillary microvasculature. Thus, relative to the very rapid time course of androgen-induced angiogenesis, the androgen-associated elevation in BDNF was delayed in onset. This suggests that the HVC vascular bed becomes receptive to VEGF by virtue of an initial gonadal steroid-mediated induction of VEGF-R2/Quek1, that it next expands in response to testosterone-induced VEGF, and that only then does the HVC capillary bed begin to provide a significant source of BDNF.

Potential Physical Interactions of New Neurons and the HVC Vascular Bed

The provision of an "angiogenic niche" for local neurogenesis has been reported in the dentate gyrus of the hippocampus, in which mitotic neurogenesis may occur concurrently with angiogenesis in pseudo-glomerular structures, in which dividing neuronal and endothelial precursor cells are directly contiguous (Palmer et al., 2000). In the adult avian brain, this concept may now be extended significantly to include the interaction of a neurogenic germinal matrix, the ventricular zone, with a noncontiguous angiogenic bed into which new neurons derived from that germinal zone migrate. In this case, the angiogenic niche provided by the activated microvascular bed includes both a spatial target for neuronal migrants as well as a source of trophic support upon their arrival. It is worth noting in this regard that in the developing telencephalon, after an initial period of radially directed migration, new neurons may leave their radial cell substrate to migrate tangentially to their targets (Walsh and Cepko, 1992; Walsh and Doherty, 1992). In the adult HVC, radial cells may terminate frequently on capillary endothelial cells (Goldman, 1995). Thus, it is possible that new neurons arriving at the angiogenic bed of the adult HVC might leave their radial cell partners to migrate upon the adluminal surfaces of the capillary microvasculature, as has been frequently observed with transplanted neural progenitor cells. Such migrants might have a ready source of neurotrophic support in BDNF secreted adluminally by the testosterone-activated endothelium. Furthermore, BDNF-secreting endothelial cells have already been observed to support the migration and survival of neurons derived from the adult rodent VZ in a trkB-dependent manner (Leventhal et al., 1999). Together, these observations suggest that endothelial cells of the adult HVC may serve to provide both humoral direction of neuronal chemotaxis and survival as well as the physical scaffolding for local parenchymal migration and dispersal.

Experimental Procedures

RNA Preparation and RT-PCR

Total RNA was extracted from dissected HVC tissue or HVC endothelial cell cultures, and equal amounts of each sample were subjected to RT-PCR as previously described (Leventhal et al., 1999). Each reaction was standardized against a G3PDH control to permit comparison between samples in each PCR. cDNA was generated using MLV reverse transcriptase (GIBCO, Rockland, ME) and amplified by the following gene-specific primers based on chicken homologs:

The primers used for RT-PCR were as follows: *vegf*, 5′-CAT GAACTTTCTGCTCTCTTG-3′ and 3′-TCTTTCTTTGGTCTGCATTCA CAT-5′; *quek1*, 5′-GGGCGTGGAGCTTTTGGTC-3′and 3′-CGTCAC TCAGGGATCGCTCTTC-5′; *bdnf*, 5′-AGCCTCCTCTGCTCTTTCTG CTGGA-3′and 3′-CTTTTGTCTATGCCCCTGCAGCCTT-5′; *G3PDH*, 5′-CCATGTTCGTCATGGGTGTGAACCA-3′ and 3′ -GCCAGTAGAG GCAGGGATGATGTTC-5′.

PCR was carried out for 35 cycles in a Perkin-Elmer 2400 thermal cycler (94°C, 45 s; 55°C, 45 s; 74°C, 45 s). The PCR products were cloned into pGEM-T (Promega) and sequenced by the Cornell Biotechnology facility in Ithaca, NY. BLAST analysis (NCBI) was per-

formed to confirm the homology of each derived sequence to known sequences.

Semiquantitative RT-PCR

RNA was extracted from pooled bilateral HVC samples at each of six time points, which included 0, 4, 8, 14, 21, and 28 days post-silastic hormone implantation (n = 3 birds/time point). RNA was extracted from pooled bilateral HVC samples, and equal amounts were subjected to [^{32}P]dCTP-reported RT-PCR, with each reaction standardized against a glucose 3-phosphate dehydrogenase (G3PD) internal control. After extraction by RNA-STAT-20, 50–200 ng of each sample was reverse transcribed using Superscript II RNase H-reverse transcriptase (GIBCO/Life Technologies) and then digested with RNase H (1 μl) for 20 min at 37°C. The cDNAs thereby generated were amplified in 50λ PCR reactions that contained 2 mM $MgCl_2$, 1× buffer, 0.2 μM primers, 0.2 μM dNTP mix, 50 ng (10 μl) RT product, 1 U red Taq polymerase, and 2.5 μCi [^{32}P]dCTP. Reactions were carried out for 24 cycles (G3PDH), 28 cycles (VEGF), or 30 cycles (BDNF) in a Perkin-Elmer 2400 thermal cycler, with denaturing at 94°C, 30 s; annealing at 55°C, 1 min; and synthesis at 72°C, 2 min. These conditions produced amplicons within the linear exponential phase of the PCR amplification curve. The resultant PCR products were then separated using PAGE and exposed to a phosphoimager cassette. The volume-density of each VEGF and BDNF band was then quantified using ImageQuant software and normalized against G3PD by dividing that time-point band density by that of its matched G3PD PCR.

In Situ Hybridization

Upon sacrifice, brains were fixed by intracardiac perfusion with cold PBS followed by 4% paraformaldehyde in PBS, followed by postfixation for 2 hr at 4°C and saturation with 30% sucrose overnight. 40 μm sections were then cut on a freezing microtome, collected in cold 0.1 M phosphate buffer (PB), cleared through alcohols to chloroform, and rehydrated in 0.1 M PB. Sections were transferred to cold 2× SSC. Prehybridization and hybridization were carried out in buffer containing 2× SSC, 50% formamide, 10% dextran sulfate, 5× Denhardt's solution, and 1 mg/ml denatured salmon sperm DNA.

Probe DNA was prepared using partial cDNA sequences for canary *vegf*, *quek1*, and *bdnf*, each obtained by reverse transcription of RNA from intestine (*vegf* and *quek1*) and brain (*bdnf*). The probes were labeled with [S^{35}]dCTP using random primer labeling (Amersham). Denatured probe was added to the prehybridization buffer and hybridized overnight. Posthybridization washes were performed in 2× SSC, 1× SSC, and 0.5× SSC at 42°C followed by a 25°C wash in 0.05 M PB. Sections were mounted on gelatin slides and either dipped in NTB2 emulsion (Kodak) or exposed to X-ray film for autoradiography.

Immunohistochemistry

For VEGF and Hu immunohistochemistry, brains were fixed by intracardiac perfusion of the animal with cold HBSS followed by 4% paraformaldehyde and postfixation and saturation with 30% sucrose. Each brain was sectioned transversely at 14 μm on a Hacker cryostat and stored frozen prior to immunohistochemistry.

Hu/BrdU

Newly generated HVC neurons were detected by staining for Hu protein, a neuronal marker (Barami et al., 1995), and BrdU using double-immunofluorescence. Hu antigen was detected using a mouse monoclonal anti-Hu IgG, 16A11 (Molecular Probes, Eugene, OR), which recognizes the Hu/Elav family members, HuC, HuD, and Hel-N1, and specifically labels neurons. The antibody was used at a concentration of 10 μg/mL. Sections were rehydrated with PBS and treated with 10 mM sodium citrate (pH 6.0) for 40 min. Sections were then permeabilized with 0.1% saponin for 15 min, blocked with 10% goat serum for 1 hr, and exposed to anti-Hu IgG overnight at 4°C. After washing, the primary anti-Hu antibody was detected with biotinylated goat anti-mouse IgG Fab (1:200), followed by a Texas red-conjugated avidin (Vector, 1:50). The sections were denatured in 2 N HCl for 30 min, then stained for BrdU using rat anti-BrdU IgG antibody at 1:200 (Harlan Sprague Dawley, Indianapolis, IN), followed serially by Alexa Fluor 488-conjugated anti-rat IgG (Molecular Probes).

VEGF

Immunoreactivity was localized using rabbit anti-VEGF165 (Neo-Markers). Slides were placed in 0.1% Triton X-100 for 30 min, washed in 0.1 M PB, exposed to 10% normal rabbit serum for 30 min, then anti-VEGF IgG at 1:200 overnight at 4°C. After washing, the slides were incubated in biotinylated goat anti-rabbit IgG (1:200; Vector Laboratories) at 25°C for 90 min, washed, incubated in avidin-biotin-HRP complex (Vectastain ABC; Vector) for 60 min, washed again, then developed with diaminobenzidine (0.2 mg/ml) and 0.003% hydrogen peroxide for 5 min. The slides were then washed, cleared through ascending alcohols and xylene, mounted in Permount, and photographed using an Olympus IX70 photomicroscope. Control slides were treated similarly except for the substitution of 1:1000 normal rabbit serum for the primary antibody; no cellular labeling was observed in these sections.

Laminin

Visualization of the vasculature was achieved using a rabbit anti-laminin IgG (Sigma). Sections were permeabilized by 0.1% saponin for 15 min, blocked with 10% goat serum for 1 hr, and exposed to anti-laminin IgG (1:100) overnight at 4°C. After washing, the primary anti-laminin antibody was detected with Alexa Fluor 566-conjugated goat anti-rabbit IgG (Molecular Probes) (1:400). Endothelial cell division was detected by staining for BrdU (see below) prior to laminin immunolabeling.

Endothelial Cell Selection, Separation, and Culture

Adult canary brain endothelial cells (CBECs) were obtained from the dissected neostriatum of adult canaries. The birds were perfused with cold HBSS via a transcardiac approach following terminal anesthesia by pentobarbital overdose. The tissue was collected in HEPES-buffered DMEM/F12 and minced into 2–4 mm^3 cubes. Isolation and preparation of endothelial cell cultures was performed using our previously described modification (Leventhal et al., 1999) of established protocols (Biegel et al., 1995). Briefly, the HVC endothelial cells were identified by their cobblestone-like morphology and binding of DiI-conjugated acetylated LDL (1,1′-dioctacecyl-3,3,3′3, tetramethyl indocarbocyanine-acetylated low density lipoprotein) (Intracel, Rockville, MD). The DiI-labeled endothelial cells were then enriched to purity using FACS. To this end, the cultures were incubated at 37°C for 1 hr with dil-acetylated LDL (1 μg/ml), washed three times in PBS, trypsinized, and resuspended in 2 ml phenol red-free medium. The endothelial dissociates were then subjected to FACS using a Becton-Dickinson FACS Vantage system, and the DiI-labeled fraction was separated at 2000–3000 cells/sec. We have previously verified, by immunolabeling for the endothelial-specific antigens factor VIII and PECAM, that >99% of DiI-LDL-bound cells sorted by this protocol are endothelial (Leventhal et al., 1999).

Upon isolation, the cells were raised in microvascular endothelial basal medium (MEBM; Sigma) supplemented with Endothelial Supplement (1×, Sigma), 20 ng/ml VEGF (Genzyme), and 20 ng/ml FGF2 (Sigma). The cells were plated on 24-well plates (Falcon Primaria) coated with human fibronectin (GIBCO, 1 μg/cm^2) at 5×10^4 cells/cm^2.

[^{3}H]Thymidine Incorporation Assay

Endothelial cells were enriched from the HVC region by FACS of DiI-LDL-tagged dissociates of adult canary HVC and adjacent mediocaudal neostriata. The cultures were raised for 2 days in MEBM medium containing 1% steroid-depleted FBS, then switched for 2 days into test media supplemented with either testosterone (100 ng/ml), β-estradiol (10 ng/ml), dihydrotestosterone (100 ng/ml), cholesterol (100 ng/ml), or VEGF (20 ng/ml), in the presence of 3.5 μCi/ml [^{3}H]thymidine. Each steroid was added either as a cyclodextran-encapsulated water-soluble formulation (Sigma: testosterone, CT5035; estradiol, E4389) or presolubilized in dimethylsulfoxide (cholesterol, 5α-dihydrotestosterone). After 2 days in test media, the cultures were extracted, and [^{3}H]thymidine incorporation was counted by a Packard 1900CA scintillation counter.

ELISA

Tissue

To quantify BDNF and VEGF protein levels, dissected tissue samples were first frozen in liquid nitrogen and then stored at −80°C. At the time of assay, the samples were thawed and lysed in 2 ml/g of tissue

of Protein Lysis Buffer (137 mM NaCl, 20 mM Tris, 1% NP-40, 10% glycerol, 1 mM PMSF, 10 μg/ml aprotinin, 0.5 mM sodium vanadate). The mixture was homogenized and centrifuged at 2500 rpm for 15 min; the supernatant was then collected and assayed either for BDNF, using Promega's BDNF ELISA, or VEGF, using R & D System's Quantikine ELISA, both according to the manufacturer's protocols.

Cells

To measure BDNF protein, confluent layers of endothelial cells in T75 flasks were homogenized in 1.5 ml buffer (50 mM Tris-HCl [pH 7.4], 600 mM NaCl, 0.2% Triton X-100, 1% BSA fraction V, 200 KIU/ml aprotonin, 0.1 mM benzethonium chloride, 1 mM benzamidine, and 0.1 mM PMSF; all from Sigma or GIBCO). Lysates were centrifuged at 10,000 × g for 30 min at 4°C, and their supernatants frozen at −80°C. Conditioned media from each sample were also frozen for ELISA. BDNF levels were then determined using a two-site ELISA (Promega) (Mizisin et al., 1997). The mouse capture antibody specifically recognized BDNF and did not cross react with other members of the neurotrophin family at concentrations up to 10,000 times that used for the standard curve. The reporter antibody was a biotinylated rabbit polyclonal anti-BDNF. The dynamic range of the ELISA was 10 pg/ml–20 ng/ml for undiluted samples; all samples were diluted in assay buffer to bring them into the linear range of the assay. Sample values were extrapolated from the standard curve, and each represented the average of triplicate samples. Total protein levels were assessed by DC protein assay (Bio-Rad).

Adult Canary VZ Explant Cultures

Culture Preparation

For neuronal outgrowth and survival studies, explants were obtained from 1-year-old female canaries (*Serinus canarius*, American Singer str., n = 5). Cultures were prepared from the neostriatal VZ, both overlying and medial to nucleus HVC, using previously reported methods and media (Goldman, 1990; Goldman et al., 1992). In brief, to phenol red-free DMEM/F12 with 15 mM HEPES, we added glutamine (2 mM), glucose (6 mg/ml), an insulin (6 μg/ml)-transferrin (6 μg/ml)-selenium (6 ng/ml) mix supplemented with linoleic acid-rich (5 μg/ml) albumin (1.25 mg/ml; ITS$^+$, Collaborative Research), hydrocortisone (300 ng/ml; water-soluble preparation, Sigma H0396), progesterone (60 fg/ml), putrescine (16 μg/ml), and tri-iodothyronine (30 ng/ml). To this base, we added charcoal-stripped fetal bovine serum (Hyclone) and castrated rooster (capon) serum (Cocalico), each at 10% v/v. The charcoal-stripped serum was assayed to contain 330 pg/ml T3 and 1.3 μU/ml insulin, each representing an approximate 80% reduction in their initial concentration (Hyclone Labs). Estradiol, testosterone, and androstenedione were all undetectable in both the stripped sera and resultant depleted medium (Mayo Clinic Labs) (see Hidalgo et al. [1995] for assay description). Each bird's explants were apportioned into treatment (BDNF, 20 ng) and control groups. Once an explant displayed cellular outgrowth, its neurons were identified using morphological criteria that we have established and verified immunocytochemically, ultrastructurally, and functionally in this system (Goldman et al., 1992). Neurons within each explant outgrowth were counted every third day beginning on day 5; one-third volume media changes were performed twice weekly, with BDNF supplementation as appropriate.

Statistical Analysis

At each time point, the mean number of neurons per explant were calculated for each treatment group (BDNF and null control). Explant growth patterns were then analyzed using two-factor analysis of variance (ANOVA). The time points (days in vitro) at which counts were made constituted the repeated measures factor, whereas the type of treatment (BDNF versus vehicle) was the main effect of the ANOVA. For statistically significant ANOVA results of $p < 0.05$, post hoc pairwise comparisons were made between treatments using a Boneferroni adjustment for multiple comparisons.

VEGF Tyrosine Kinase Inhibition

4-[(4′-Chloro-2′-fluoro)phenylamino]-6,7-dimethoxyquinazoline (VEGFR Tyrosine Kinase Inhibitor, Calbiochem No. 676475) was used to inhibit VEGF-dependent angiogenesis according to the experimental design described above in the Results. This inhibitor is the fourth of a series of anilinoquinazolines synthesized as potent inhibitors of VEGF receptor tyrosine kinase activity (IC_{50} = 0.1 μM for VEGF-R2 and 2.0 μM for VEGF-R1/flt1) (Hennequin et al., 1999). The substituted halogens and its methoxy groups at C6 and C7 made this particular anilinoquinazoline both more potent and the most likely of the series to cross the blood brain barrier based on lipophobicity.

Confocal Imaging

In sections double-stained for BrdU and Hu, single BrdU$^+$ cells that appeared double-labeled with Hu were further evaluated by confocal imaging. Using a Zeiss LSM510 microscope, images were acquired in both red and green emission channels using an argon-krypton laser. The images were then viewed as series of single 0.9 μm optical sections and as merged z-dimension composites thereof. The z-dimension reconstructions were observed in profile, as every BrdU$^+$/Hu$^+$ cell was observed orthogonally in both the vertical and horizontal planes. Cells were scored as double-labeled, newly generated neurons only when observed to have central BrdU immunoreactivity surrounded by Hu-immunoreactivity in every serial optical section and in each rotated orthogonal view, as previously described (Benraiss et al., 2001).

Scoring

Capillary Parameters

In each sampled HVC, every laminin$^+$ profile within the cresyl-defined borders of HVC was traced and recorded manually into BioQuant image analysis software. A profile was defined as the net surface area of laminin immunolabeling. Capillary counts were derived from these profiles, and no correction was made for tangential cuts. This was based upon an assumption of randomly distributed capillary orientations in HVC coronal sections. Each traced outline was then analyzed for its area, perimeter, and diameter, and the average numbers per HVC and per unit area were determined. Statistical analysis between treatment groups was then accomplished by ANOVA followed by post hoc Boneferroni t tests.

Endothelial Labeling Indices

For the evaluation of testosterone-induced angiogenesis, the brains of six birds were cryosectioned at 14 μm and double-immunostained for BrdU together with laminin. In each nucleus HVC, the incidence of laminin$^+$/BrdU$^+$ cells and the ratio of laminin$^+$/BrdU$^+$ cells to total HVC laminin$^+$ ECs were determined bilaterally in each of six sections spaced 200 μm apart. Total HVC endothelial cells were counted by double-labeling laminin-stained sections with the nuclear dye Hoechst 33258 so as to visualize and score individual endothelial nuclei.

Neuronal Labeling Indices

For the VEGF TKI inhibition study, five 14 μm sections were chosen from each of 14 birds. These were taken at intervals of 100 μm spanning the nucleus HVC through the antero-posterior coordinates A0.0 to P0.6 in the stereotaxic plane (Stokes et al., 1976). Each sampled slide included both hemispheres, roughly symmetrical in the coronal plane at the level of HVC. HVC was delineated in each hemisphere by cresyl violet Nissl staining in adjacent sections. The total number of Hu$^+$ neurons and double-positive Hu$^+$/BrdU$^+$ neurons were scored in the ten HVC samples analyzed per bird. The percentage of HVC Hu$^+$ neurons that were double-labeled for BrdU was determined for each bird, and the group means, standard deviations, and errors were then calculated. The group means were then compared by two-way ANOVA, with post hoc comparisons by Bonferroni t tests. Comparisons were considered significant for $p \leq 0.05$.

Acknowledgments

Supported by the G. Harold and Leila Y. Mathers Charitable Foundation, NINDS R37/R01NS29813 and R01NS33106, the National Multiple Sclerosis Society, and Project ALS. A.L. was supported by NIH MSTP grant GM07739 and the Friedman Fellowship Endowment. We are grateful to Drs. George Yancopoulos, Stan Wiegand, and Anne Acheson of Regeneron Pharmaceuticals for BDNF protein, cDNA, and for sharing their ELISA protocols. We thank Dr. Marcus Reidenberg for advice on the use of VEGF tyrosine kinase inhibitors, Drs. Francis Barany and Abdellatif Benraiss for advice on relative PCR, and Donna Roh for technical assistance.

Received: March 20, 2001
Revised: April 15, 2002

References

Alitalo, K., Kurkinen, M., Virtanen, I., Mellstrom, K., and Valheri, A. (1982). Deposition of basement membrane proteins in attachment and neurite formation of cultured murine C-1300 neuroblastoma cells. J. Cell. Biochem. *18*, 25–36.

Alvarez-Buylla, A., and Nottebohm, F. (1988). Migration of young neurons in adult avian brain. Nature *335*, 353–354.

Andersson, C., Lydrup, M.-L., Ferno, M., Idvall, I., Gustafsson, J.-A., and Nilsson, B. (2001). Immunocytochemical demonstration of oestrogen receptor-beta in blood vessels of the female rat. J. Endocrinol. *169*, 241–247.

Araujo, D., and Cotman, C. (1993). Trophic effects of interleukin-4, -7 and -8 on hippocampal neuronal cultures: potential involvement of glial-derived factors. Brain Res. *600*, 49–55.

Balthazart, J., Absil, P., Foidart, A., Houbart, M., Harada, N., and Ball, G. (1996). Distribution of aromatase-immunoreactive cells in the forebrain of zebra finches: implications for the neural action of steroids. J. Neurobiol. *31*, 129–148.

Barami, K., Kirschenbaum, B., Lemmon, V., and Goldman, S.A. (1994). N-cadherin and Ng-CAM/8D9 are involved serially in the migration of newly generated neurons into the adult songbird brain. Neuron *13*, 567–582.

Barami, K., Iversen, K., Furneaux, H., and Goldman, S.A. (1995). Hu protein as an early marker of neuronal phenotypic differentiation by subependymal zone cells of the adult songbird forebrain. J. Neurobiol. *28*, 82–101.

Behar, T., Dugich-Djordjevic, M.M., Li, Y.X., Ma, W., Somogyi, R., Wen, X., Brown, E., Scott, C., McKay, R.D., and Barker, J.L. (1997). Neurotrophins stimulate chemotaxis of embryonic cortical neurons. Eur. J. Neurosci. *9*, 2561–2570.

Benraiss, A., Chmielnicki, E., Roh, D., and Goldman, S.A. (2001). Adenoviral BDNF induces both neostriatal and olfactory neuronal recruitment from endogenous progenitor cells in the adult forebrain. J. Neurosci *21*, 6718–6731.

Bergers, G., Brekken, R., McMahon, G., Vu, T., Itoh, T., Tmaki, K., Tanzawa, K., Thorpe, P., Itohara, S., Werb, Z., et al. (2000). Matrix metalloproteinase-9 triggers the angiogenic switch during carcinogenesis. Nat. Cell Biol. *2*, 737–744.

Bernard, D., Bentley, G., Balthazart, J., Turek, F., and Ball, G. (1999). Androgen receptor, estrogen receptor alpha, and estrogen receptor beta show distinct patterns of expression in forebrain song control nuclei of European starlings. Endocrinology *140*, 4633–4643.

Biegel, D., Spencer, D.D., and Pachter, J.S. (1995). Isolation and culture of human brain microvascular endothelial cells for the study of blood-brain barrier properties in vitro. Brain Res. *692*, 183–189.

Biro, S., Yu, Z., Fu, Y., Smale, G., Sasse, J., Sanchez, J., Ferrans, V., and Casscells, W. (1994). Expression and subcellular distribution of basic fibroblast growth factor are regulated during migration of endothelial cells. Circ. Res. *74*, 485–494.

Bottjer, S., and Johnson, F. (1997). Circuits, hormones, and learning: vocal behavior in songbirds. J. Neurobiol. *33*, 602–618.

Breier, G., Albrecht, U., Sterrer, S., and Risau, W. (1992). Expression of vascular endothelial growth factor during embryonic angiogenesis and endothelial cell differentiation. Development *114*, 521–532.

Caulin-Glaser, T., Watson, C., Pardi, R., and Bender, J. (1996). Effects of 17β-estradiol on cytokine-induced endothelial cell adhesion molecule expression. J. Clin. Invest. *98*, 36–42.

Dittrich, F., Feng, Y., Metzdorf, R., and Gahr, M. (1999). Estrogen-inducible, sex-specific expression of BDNF mRNA in a forebrain song control nucleus of the juvenile zebra finch. Proc. Natl. Acad. Sci. USA *96*, 8241–8246.

Drago, J., Murphy, M., Carroll, S.M., Harvey, R.P., and Bartlett, P.F. (1991). Fibroblast growth factor-mediated proliferation of central nervous system precursors depends on endogenous production of insulin-like growth factor I. Proc. Natl. Acad. Sci. USA *88*, 2199–2203.

Fusani, L., Hutchison, J., and Gahr, M. (2001). Testosterone regulates the activity and expression of aromatase in the canary neostriatum. J. Neurobiol. *49*, 1–8.

Gahr, M. (1990). Delineation of a brain nucleus: comparisons of cytochemical, hodological, and cytoarchitectural views of the song control nucleus HVC of the adult canary. J. Comp. Neurol. *294*, 30–36.

Gensburger, C., Labourdette, G., and Sensenbrenner, M. (1987). Brain basic fibroblast growth factor stimulates the proliferation of rat neuronal precursor cells in vitro. FEBS Lett. *217*, 1–5.

Goldman, S.A. (1990). Neuronal development and migration in explant cultures of the adult canary forebrain. J. Neurosci. *10*, 2931–2939.

Goldman, S.A. (1995). Neuronal precursor cells and neurogenesis in the adult forebrain. Neuroscientist *1*, 338–350.

Goldman, S.A. (1998) Adult neurogenesis: from canaries to the clinic. J. Neurobiol. *36*, 267–286.

Goldman, S.A., and Luskin, M.B. (1998). Strategies utilized by migrating neurons of the postnatal vertebrate forebrain. Trends Neurosci. *21*, 107–114.

Goldman, S.A., and Nottebohm, F. (1983). Neuronal production, migration, and differentiation in a vocal control nucleus of the adult female canary brain. Proc. Natl. Acad. Sci. USA *80*, 2390–2394.

Goldman, S.A., Zaremba, A., and Niedzwiecki, D. (1992). In vitro neurogenesis by neuronal precursor cells derived from the adult songbird brain. J. Neurosci. *12*, 2532–2541.

Hanahan, D. (1997). Signaling vascular morphogenesis and maintenance. Science *277*, 48–50.

Hennequin, L.F., Thomas, A.P., Johnstone, C., Stokes, E.S., Plé, P.A., Lohmann, J.J., Ogilvie, D.J., Dukes, M., Wedge, S.R., Curwen, J.O., et al. (1999). Design and structure-activity relationship of a new class of potent VEGF receptor tyrosine kinase inhibitors. J. Med. Chem. *42*, 5369–5389.

Hidalgo, A., Barami, K., Iversen, K., and Goldman, S.A. (1995). Estrogens and non-estrogenic ovarian influences combine to promote the recruitment and decrease the turnover of new neurons in the adult female canary brain. J. Neurobiol. *27*, 470–487.

Holzenberger, M., Jarvis, E., Chong, C., Grossman, M., Nottebohm, F., and Scharff, C. (1997). Selective expression of insulin-like growth factor II in the songbird brain. J. Neurosci. *17*, 6974–6987.

Iafrati, M.D., Karas, R.H., Aronovitz, M., Kim, S., Sullivan, T.R., Jr., Lubahn, D.B., O'Donnell, T.F. Jr., Korach. K.S., and Mendelsohn, M.E. (1997). Estrogen inhibits the vascular injury response in estrogen receptor α-deficient mice. Nat. Med. *3*, 545–548.

Jain, R., Safabakhsh, N., Sckell, A., Chen, Y., Jiang, P., Benjamin, L., Yuan, F., and Keshet, E. (1998). Endothelial cell death, angiogenesis, and microvascular function after castration in an androgen-dependent tumor: role of VEGF. Proc. Natl. Acad. Sci. USA *95*, 10820–10825.

Jiang, W., McMurtry, J., Niedzwiecki, D., and Goldman, S.A. (1998). Insulin-like growth factor-1 is a radial cell-associated neurotrophin that promotes neuronal recruitment from the adult songbird ventricular zone. J. Neurobiol. *36*, 1–15.

Johe, K.K., Hazel, T.G., Muller, T., Dugich-Djordjevic, M.M., and McKay, R.D. (1996). Single factors direct the differentiation of stem cells from the fetal and adult central nervous system. Genes Dev. *10*, 3129–3140.

Johnson, F., and Bottjer, S. (1995). Differential estrogen accumulation among populations of projection neurons in the higher vocal center of male canaries. J. Neurobiol. *26*, 87–108.

Kirschenbaum, B., and Goldman, S.A. (1995). Brain-derived neurotrophic factor promotes the survival of neurons arising from the adult rat forebrain subependymal zone. Proc. Natl. Acad. Sci. USA *92*, 210–214.

Legan, S., Coon, G., and Karsch, F. (1975). Role of estrogen as initiator of daily LH surges in the ovariectomized rat. Endocrinology *96*, 50–56.

Leung, D., Cachianes, G., Kuang, W., Goeddel, D., and Ferrara, N.

(1989). Vascular endothelial growth factor is a secreted angiogenic mitogen. Science *246*, 1306–1309.

Leventhal, C., Rafii, S., Rafii, D., Shahar, A., and Goldman, S.A. (1999). Endothelial trophic support of neuronal production and recruitment from the adult mammalian subependyma. Mol. Cell. Neurosci. *13*, 450–464.

Levine, A., Liu, X., Greenberg, P., Eliashvili, M., Schiff, J., Aaronson, S., Holland, J., and Kirschenbaum, A. (1998). Androgens induce the expression of VEGF in human fetal prostatic fibroblasts. Endocrinology *139*, 4672–4678.

Li, X., Jarvis, E., Alvarez-Borda, B., Lim, D., and Nottebohm, F. (2000). A relationship between behavior, neurotrophin expression, and new neuron survival. Proc. Natl. Acad. Sci. USA *97*, 8584–8589.

Lindner, V., Kim, S., Karas, R., Kuiper, G., Gustafsson, J., and Mendelsohn, M. (1998). Increased expression of estrogen receptor β mRNA in male blood vessels after vascular injury. Circ. Res. *83*, 224–229.

Millauer, B., Wizigmann, S., Schnurch, H., Martinez, R., Moller, N., Risau, W., and Ullrich, A. (1993). High-affinity VEGF binding and developmental expression suggest FLk-1 as a major regulator of vasculogenesis and angiogenesis. Cell *72*, 835–846.

Mizisin, A.P., Bache, M., DiStefano, P.S., Acheson, A., Lindsay, R.M., and Calcutt, N.A. (1997) BDNF attenuates functional and structural disorders in nerves of galactose-fed rats. J. Neuropathol. Exp. Neurol. *56*, 1290–1301.

Mosselman, S., Polman, J., and Dijkema, R. (1996). ERβ: identification and characterization of a novel human estrogen receptor. FEBS Lett. *392*, 49–53.

Mueller, M., Vigne, J., Minchenko, A., Lebovic, D., Leitman, D., and Taylor, R. (2000). Regulation of VEGF gene transcription by estrogen receptors α and β. Proc. Natl. Acad. Sci. USA *97*, 10972–10977.

Nag, S., Takahashi, J., and Kilty, D. (1997). Role of VEGF in blood-brain barrier breakdown and angiogenesis in brain trauma. J. Neuropathol. Exp. Neurol. *56*, 912–921.

Nastiuk, K., and Clayton, D. (1995). The canary androgen receptor mRNA is localized in the song control nuclei of the brain and is rapidly regulated by testosterone. J. Neurobiol. *26*, 213–224.

Nordeen, E., and Nordeen, K. (1989). Estrogen stimulates the incorporation of new neurons into avian song nuclei during adolescence. Brain Res. Dev. Brain Res. *49*, 27–32.

Nottebohm, F. (1981). A brain for all seasons: cyclical anatomical changes in song control nuclei of the canary brain. Science *214*, 1368–1370.

Nottebohm, F. (1985). Neuronal replacement in adulthood. Ann. N Y Acad. Sci. *457*, 143–161.

Ogunshola, O., Stewart, W., Mihalcik, V., Solli, T., Madri, J., and Ment, L. (2000). Neuronal VEGF expression correlates with angiogenesis in postnatal developing rat brain. Brain Res. Dev. Brain Res. *119*, 139–153.

Ogunshola, O., Antic, A., Donoghue, M.J., Fan, S.Y., Kim, H., Stewart, W.B., Madri, J.A., and Ment, L.R. (2002). Paracrine and autocrine functions of neuronal VEGF in the CNS. J. Biol. Chem. *277*, 11410–11415.

Palmer, T., Willhoite, A., and Gage, F. (2000). Vascular niche for adult hippocampal neurogenesis. J. Comp. Neurol. *425*, 479–494.

Pardridge, W. (1995). Transport of small molecules through the blood-brain barrier: biology and methodology. Adv. Drug Deliv. Rev. *15*, 5–36.

Proescholdt, M., Heiss, J., Walbridge, S., Muhlhauser, J., Oldfield, E., and Merrill, M. (1999). VEGF modulates vascular permeability and inflammation in the rat brain. J. Neuropathol. Exp. Neurol. *58*, 613–627.

Rasika, S., Nottebohm, F., and Alvarez-Buylla, A. (1994). Testosterone increases the recruitment and/or survival of new high vocal center neurons in adult female canaries. Proc. Natl. Acad. Sci. USA *89*, 8591–8595.

Rasika, S., Alvarez-Buylla, A., and Nottebohm, F. (1999). BDNF mediates the effects of testosterone on the survival of new neurons in an adult brain. Neuron *22*, 53–62.

Robertson, P., Du Bois, M., Bowman, P., and Goldstein, G. (1985). Angiogenesis in the developing rat brain: an in vivo and in vitro study. Brain Res. *23*, 219–223.

Rosenstein, J., Mani, N., Silverman, W., and Krum, J. (1998). Patterns of brain angiogenesis after vascular endothelial growth factor administration in vitro and in vivo. Proc. Natl. Acad. Sci. USA *95*, 7086–7091.

Shen, P., Schlinger, B., Campagnoni, A., and Arnold, A. (1995). An atlas of aromatase mRNA expression in the zebra finch brain. J. Comp. Neurol. *360*, 172–184.

Soker, S., Takashima, S., Miao, H., Neufeld, G., and Klagsbrun, M. (1998). Neuropilin-1 is expressed by endothelial and tumor cells as an isoform-specific receptor for VEGF. Cell *92*, 735–745.

Stokes, T., Leonard, C., and Nottebohm, F. (1976). The telencephalon, diencephalon and mesencephalon of the canary, *Serinus canaria*, in stereotaxic coordinates. J. Comp. Neurol. *156*, 337–374.

Suri, C., Jones, P., Patan, S., Bartunkova, S., Maisonpierre, P., Davis, S., Sato, T., and Yancopoulos, G. (1996). Requisite role of angiopoetin-1, a ligand for the TIE2 receptor, during embryonic angiogenesis. Cell *87*, 1171–1180.

Suri, C., McClain, J., Thurston, G., McDonald, D., Zhou, H., Oldmixon, E., Sato, T., and Yancopoulos, G. (1998). Increased vascularization in mice overexpressing angiopoiein-1. Science *282*, 468–471.

Thurston, G., Suri, C., Smith, K., McClain, J., Sato, T., Yancopoulos, G., and McDoanld, D. (1999). Leakage-resistant blood vessels in mice transgenically overexpressing angiopoietin-1. Science *286*, 2511–2514.

Walsh, C., and Cepko, C.L. (1992). Widespread dispersion of neuronal clones across functional regions of the cerebral cortex. Science *255*, 434–440.

Walsh, F., and Doherty, P. (1992). Second messengers underlying cell-contact dependent axonal growth stimulated by transfected N-CAM, N-cadherin, or L1. Cold Spring Harb. Symp. Quant. Biol. *57*, 431–440.

Wedge, S., Ogilvie, D., Dukes, M., Kendrew, J., Curwen, J., Hennequin, L., Thomas, A., Stokes, E., Curry, B., Richmond, G., and Wadsworth, P. (2000). ZD4190: an orally active inhibitor of VEGF signaling with broad-spectrum antitumor efficacy. Cancer Res. *60*, 970–975.

Wilting, J., Eichmann, A., and Christ, B. (1997). Expression of the avian VEGF recptor homologues Quek1 and Quek2 in blood-vascular and lymphatic endothelial and non-endothelial cells during quail embryonic development. Cell Tissue Res. *288*, 207–223.

Yancopoulos, G., Davis, S., Gale, N., Rudge, J., Wiegand, S., and Holash, J. (2000). Vascular-specific growth factors and blood vessel formation. Nature *407*, 242–248.

Yang, X, and Cepko, C. (1996). Flk-1, a receptor for vascular endothelial growth factor (VEGF), is expressed by retinal progenitor cells. J. Neurosci. *16*, 6089–6099.

Zhang, Z., Zhang, L., Jiang, Q., Davies, K., Powers, C., van Bruggen, N., and Chopp, M. (2000). VEGF enhances angiogenesis and promotes blood–brain barrier leakage in the ischemic brain. J. Clin. Invest. *106*, 829–838.

Zigova, T., Pencea, V., Wiegand, S., and Luskin, M. (1998). Intraventricular administration of BDNF increases the number of newly generated neurons in the adult olfactory bulb. Mol. Cell. Neurosci. *11*, 234–245.